NATIONAL ADVISORY COMMITTEE FOR AERONAUTICS

MEMORANDUM REPORT

for the

Army Air Forces, Air Technical Service Command

FLIGHT TESTS OF THE HIGH-SPEED PERFORMANCE OF A P-51B AIRPLANE (AAF NO. 43-12105)

By T. J. Vogelwede and E. C. B. Danforth

Langley Memorial Aeronautical Laboratory
Langley Field, Va.

December 18, 1944

MR No. L4L18 [redacted]

NATIONAL ADVISORY COMMITTEE FOR AERONAUTICS

MEMORANDUM REPORT

for the

Army Air Forces, Air Technical Service Command

FLIGHT TESTS OF THE HIGH-SPEED PERFORMANCE OF A P-51B AIRPLANE (AAF NO. 43-12105)

By T. J. Voglewede and E. C. B. Danforth

SUMMARY

Results of tests on a P-51B airplane in the full-scale tunnel showed that an increase in maximum speed of 3 or 4 miles per hour could be realized as a result of sealing the wing-gun access doors and flap-spar lightening holes. Flight tests on the same airplane were made to check wind-tunnel results. Because of inconsistent variations in speed of a greater mangnitude at the same altitude and with the same estimated engine power, no such small increase in speed could be isolated. In an effort to explain these variations in speed, considerably more testing and analysis were carried out.

This further study showed that near the maximum level-flight speed a sudden rise in C_D/η (ratio of airplane drag coefficient to propulsive efficiency) occurred that could be explained either by an increase in drag coefficient or a decrease in propeller efficiency. It is shown that such an abrupt increase in drag coefficient is unlikely and that this effect is more probably due to rapidly decreasing propeller efficiency. Because no torquemeter was available for these tests, the value of the flight-test data as a measure of changes in drag coefficient or propeller efficiency was considerably reduced by apparent inaccuracy in estimates of engine power. In spite of this limitation, however, the analysis of the data does indicate that appreciable losses in propeller efficiency were encountered in the maximum level-flight-speed condition near high blower critical altitude.

[redacted]

INTRODUCTION

At the request of the Army Air Forces, Air Technical Service Command, flight tests were conducted by the National Advisory Committee for Aeronautics to check the improvement of 3 or 4 miles per hour in the maximum speed of the P-51B airplane that was indicated by full-scale tunnel tests (reference 1) to be the result of sealing the wing-gun access doors and flap-spar lightening holes. Because of large arbitrary variations in speed at the same altitude and with the same estimated engine power, it was not possible to measure any such small improvement. In an attempt to find the causes of these variations in speed, airplane polars were made at 5000, 10,000, 20,000, and 31,000 feet, and an extensive analysis of the test data was undertaken with a view to isolation of the effects of various factors suspected of contributing to the inconsistency of the airplane's performance. The test data and analysis are presented herein.

AIRPLANE

General views of the P-51B airplane are shown in figures 1 to 5. The long airspeed boom on the right wing was removed for all of the speed test flights. Additional data pertinent to the tests are as follows:

1. Gross weight at take-off including 180 gallons of gas, 8840 pounds.

2. Engine; Packard-built Rolls Royce, model V-1650-3, A.F. No. 43-49089.

3. Carburetor; Bendix-Stromberg PD18A-1, parts list No. 395200-6 except with No. 47 bleed in density compensating system, Serial No. 142204.

4. Propeller; Hamilton-Standard J6487-24, four blades, 11 feet 2 inches in diameter. (See fig. 1.)

5. Wing-gun ports and wing-rack fittings taped over as shown in figure 6.

6. Free-air resistance bulb thermometer installed on under surface of wing. (See figs. 6 and 7.)

7. Special short-boom airspeed head in front of left wing. (See fig. 7.)

8. Service airspeed head under right wing. (See general views.)

9. Wing surface smoothed to the extent of eliminating accidental scratches and blemishes acquired after manufacture. Prior to flights 5, 8, and 11 the wing was carefully refinished, putting glazing putty in cracks and dents and removing protuberances with sand paper.

10. For flights 5, 6, and 7 the wing-gun access doors and the flap-spar lightening holes were not sealed. Prior to flight 8, cellulose tape was placed over the wing-gun access doors and fabric was doped over the flap-spar lightening holes. All subsequent flights were made with this configuration.

APPARATUS

Special equipment installed for these tests included synchronized NACA pressure recorders for airspeed, altitude, manifold pressure, and carburetor metering pressures; control-position recorders on coolant and oil shutters; recording revolution counter for engine speed; limit switches on the front of the wheel-well closures connected to lights in the cockpit; thermocouples and indicators for manifold temperatures before and after the aftercooler, and large sensitive indicating altimeter and sensitive airspeed indicator.

Oil and coolant temperatures were measured with the service installations.

Free-air temperatures were measured with the free-air resistance bulb thermometer (figs. 6 and 7) installed on the lower surface of the left wing. To establish the rise in temperature indication due to forward speed, the installation was calibrated in flight at altitudes of 5000 and 30,000 feet. The rise obtained was approximately 70 percent of the theoretical adiabatic rise and was independent of altitude (fig. 8).

The airspeed head used for these tests consisted of a Kollsman head mounted with the static holes 0.35 chord length ahead of the wing (fig. 7). The drain hole in the head was plugged to remove the small error in total head due to this cause. The position error of the static side of the head was calibrated by observation of the altimeter in flights at different speeds past a reference landmark of known elevation. Tests were made to determine the variation in the position error with altitude because of the change in the pressure field forward of the stagnation point of the wing with a change in free-stream Mach number at a constant indicated airspeed. Another boom with the static orifices 0.94 chord ahead of the wing was installed for these tests to measure a reference static pressure. Static pressures at this station show negligible changes with changes in Mach number (reference 2). Figure 9 shows the position error determined at sea level and also the error at 5000 and 30,000 feet. Tunnel data (reference 2) were used as a guide to fair the flight test points. The correction increased with altitude but at 30,000 feet amounted to only 1.4 miles per hour at the highest level-flight speed.

TESTS

The test program consisted of level-flight, high-speed runs at military-rated power (61 in. Hg at 3000 rpm) or full throttle at pressure altitudes ranging from 29,000 to 33,000 feet and speed-power polars at 3000 rpm at pressure altitudes of 5000, 10,000, 20,000, and 31,000 feet. Above 25,500 feet the engine was operated in high blower and below 25,500 feet in low blower. In addition, one flight was made in high and low blower at 25,500 feet and one flight at 3000 and 2700 rpm at 31,000 feet. The airplane was in the high-speed condition throughout, flap and gear up, with the prestone shutter set at 7.9 inches gap (distance from the fuselage to the trailing edge of the shutter). The oil shutter control was set in automatic and the carburetor mixture control was set in automatic rich for all runs.

Records were taken only after allowing several minutes to be certain of reaching stabilized conditions. The pilot maintained constant altitude and airspeed as closely as possible by reference to a large sensitive altimeter and a sensitive airspeed indicator.

SYMBOLS

A	aspect ratio of wing
BHP	engine brake horsepower
ΔHP	exhaust jet thrust horsepower estimated according to reference 4 minus horsepower required to stop the incoming charge air relative to the airplane
C_D	airplane drag coefficient, $C_{D_o} + \frac{C_L^2}{\pi Ae}$
C_{D_o}	assumed profile-drag coefficient at zero lift
$\left(\frac{\eta}{C_D S}\right)^{1/3}$	aerodynamic refinement parameter
C_L	airplane lift coefficient
C_p	power coefficient, $\frac{550\ BHP}{\rho n^3 D^5}$
D	propeller diameter, feet
d	engine cylinder diameter, inches
e	airplane efficiency factor
FHP	engine friction horsepower
g	acceleration of gravity, feet per second per second
IHP	engine indicated horsepower
l	stroke, inches
N	engine speed, rpm
n	propeller rotational speed, rps
n_c	number of cylinders
η	propulsive efficiency
P_1	pressure at carburetor top deck, inches of mercury
P_{man}	manifold pressure, inches of mercury

P_S	static pressure of free stream
P_S'	static pressure registered by airspeed head
P_T	total pressure of free stream
ΔP	$P_S' - P_S$
Δp	pressure drop from carburetor top deck to boost venturi throat, inches of mercury
PHP	pumping power of engine; relative net power output of induction and exhaust strokes
q_c	true impact pressure of free stream
q_c'	measured impact pressure of free stream
S	wing area, square feet
SHP	horsepower absorbed by supercharger
T	ambient free-air temperature
T_r	observed free-air temperature
ΔT	$T_r - T$
T_1	air temperature at carburetor top deck, ^oF
V	true speed, miles per hour
V_d	engine displacement, cubic feet
V_t	tip speed of supercharger inpeller, feet per second
W_a	weight charge air flow, pounds per hour
W_c	weight charge flow, pounds per hour
ω	specific weight of charge air at carburetor top deck, pounds per cubic foot
ρ	free-air density, slugs/per cubic foot
σ	free-air density ratio

RESULTS AND DISCUSSION

Engine Power

Because no torquemeter was available for these tests, the engine power was estimated from Wright Field power charts (reference 3) at the manifold pressure, engine speed, and pressure altitude of the test. The measured manifold temperature varied widely under apparently identical conditions and in such a way that the effect of the measured differences in speed was exaggerated by the apparent change in power. To avoid using these erratic manifold temperature readings, the chart power was corrected by the square root of the ratio of standard free-air temperature to observed carburetor-air temperature. The assumption of constant aftercooler effectiveness with constant shutter position was necessary. When chart power is used hereafter, it is to be understood that the carburetor-air temperature correction is involved.

When the data were reduced using this chart power, certain peculiarities were in evidence which could have arisen from errors in estimates of power. A comparison of the power estimates with the measured weight air flow to the engine brought out the fact that near full power in high blower at 3000 rpm the specific air consumption increased far more rapidly than could be accounted for by the changes in fuel-air ratio. Furthermore, specific air consumption was different for high and low blower operation after the difference in supercharger power was allowed for (fig. 10).

It was expected that an estimate of power based on measured charge weight air flow might remove some of the peculiarities noted in the data based on chart power. The direct measurement of charge weight air flow, however, produced no more logical results. Because neither method of power estimation is satisfactory in all respects, the following analysis is made with regard to both methods.

In the appendix there is given a discussion of the method of measuring the charge weight air flow and its use in the estimation of engine power.

EFFECTS OF IMPORTANT FACTORS ON SPEED

In order to determine the effect of changes in a given airplane, it is convenient to express the power-drag relationship in the form

$$V = 52.73 \left(\frac{BHP + \frac{\Delta HP}{\eta}}{\sigma} \right)^{1/3} \left(\frac{\eta}{C_D S} \right)^{1/3}$$

where

V true speed, miles per hour

BHP engine brake horsepower

ΔHP exhaust jet thrust power estimated according to reference 4 minus horsepower required to stop the incoming charge air relative to the airplane

σ free-air density ratio

η propulsive efficiency

C_D airplane drag coefficient

S wing area, square feet

In this form, speed is directly proportional to two parameters; the first, $\left(\frac{BHP + \frac{\Delta HP}{\eta}}{\sigma} \right)^{1/3}$, measures the contribution of the engine, supercharger, air scoop, and exhaust jets; the second, $\left(\frac{\eta}{C_D S} \right)^{1/3}$, is a measurement of the aerodynamic refinement of the airplane and propeller. Since the propulsive efficiency enters into the power parameter, the aerodynamic refinement parameter is not entirely independent. At the highest altitudes for this airplane, however, the magnitude of the $\Delta HP/\eta$ term is never greater than 17 percent of the whole power parameter, assuming a propulsive efficiency of 80 percent. An overestimate of propulsive efficiency of 10 percent would therefore decrease the power estimate and the value of $C_D S/\eta$ by 2.5 percent.

The high-speed data are presented in figures 11 and 12. It is seen that the $\left(\frac{\eta}{C_D S}\right)^{1/3}$ values are widely separated for different flights. The effect of the wing seals on the aerodynamic refinement could not be ascertained since both configurations show the same wide variation.

The possibility that deterioration of the wing surface might account for the change in aerodynamic refinement was investigated. Before flights 5 and 8, which show the higher $\left(\frac{\eta}{C_D S}\right)^{1/3}$ values, the wing surface was filled and sanded. Before flights 6 and 7, and 9 and 10, no additional filling was done, but the wing was wiped off and any protuberances were sanded smooth. Before flight 11, special care was taken in refinishing the wing in an effort to regain the higher speeds of flights 5 and 8, but the $\left(\frac{\eta}{C_D S}\right)^{1/3}$ values were again in the lower group. Other than keeping the wing free from dirt and protuberances, no refinishing was done after flight 11 and no further decrease in aerodynamic refinement was noted. In view of the care taken with the wing finish, it was considered unlikely that the condition of the wing surface was responsible for the large changes in speed and aerodynamic refinement, especially since the indicated spread of 9 percent in $(C_D S/\eta)$ would require about 27 percent change in the profile drag of the wing alone.

The possibility of a progressive loss in power output of the engine which would not be reflected in the air flow or manifold pressure measurements was also investigated. The spark plugs were replaced and the ignition timing and valve clearances were adjusted to the optimum conditions after flight 11. Speed and aerodynamic refinement remained the same on the subsequent flight, flight 12. As a further check on its power output, the engine was returned to the Packard Motor Company for duplication of the original run-in tests. The results of these tests are presented in table I. No significant change in engine power was noted in the check runs at those power conditions for which data were available from the original run-in tests.

Because both the speed and the power estimates depend on the measured value of free-air temperature, it was considered possible that random errors in the temperature could account for the inconsistent values of aerodynamic cleanness shown in figures 11 and 12. The temperature installation was checked on the ground for the effect of ambient temperature on the indicator. Similar resistance bulbs were mounted at several other points on the airplane for comparison in flight. The reading of one resistance bulb was checked against an alcohol thermometer during the same flight tests. These checks revealed no possibility of random error in temperature greater than 2° F. Errors of the order of 10° F would be necessary to account for the spread of aerodynamic cleanness shown in figures 11 and 12. The variation of free-air temperature with altitude observed during the initial portion of the test program is shown in figure 13.

Airplane polars.- A series of tests was made at 31,000 feet at 3000 rpm and varying throttle openings in an attempt to define the variation in aerodynamic cleanness at and near the maximum speed condition. Comparative tests were also made at lower altitudes. The data are presented in figures 14 to 19. Airplane polars were constructed by plotting C_DS/η, the inverse cube of the aerodynamic refinement parameter, against the square of the lift coefficient. For the portion of the speed range shown in the figures, airplane drag coefficient should vary linearly with the square of the lift coefficient. The dotted line in figures 14 and 15 shows the variation that might normally be expected with a profile-drag coefficient at zero lift of 0.017, a constant propeller efficiency of 0.80, and an airplane efficiency factor of 0.85.

The data in figures 14 and 15 depart from the expected values both in magnitude and in slope. The unreasonable values of C_DS/η at low speeds at each altitude indicate that the power estimates are too low in this region. The increase in C_DS/η as the speed and power are increased may also be due to inaccuracy in the estimate of power but several trends are present which lead to the belief that other causes are also present.

The rapid rise in C_DS/η near full throttle at 31,000 feet shown in figure 14 and to a lesser degree in figure 15 could be ascribed wholly to inaccuracy in

estimation of engine power only if the engine did not respond normally to increases in air flow and manifold pressure near full throttle. Whatever the reason for this rapid rise in C_DS/η, it seems logical to expect variations in speed such as are shown in the maximum speed measurements of figures 11 and 12 when operating in this region if the conditions of operation are changed slightly. The test points of figures 11 and 12 at 31,000 feet pressure altitude are replotted in figures 14 and 15 for comparison. The displacement of these latter points toward lower lift coefficients is due to differences in weight because of gasoline consumption.

The general trends of the polars in figures 14 and 15 are what would be expected if the drag coefficient were increasing or the propeller efficiency decreasing with increase in Mach number; that is, the values of C_DS/η increase as the speed increases and as the altitude increases. Because a portion of the increase in C_DS/η is due to inadequate power measurement and is not defined, it is difficult to draw conclusions concerning the remaining portion. It is more probable, however, that a rise in C_DS/η accompanying an increase in Mach number would be caused by a loss in propeller efficiency with the propeller operating at tip Mach numbers up to 1.07 rather than a rise in airplane drag coefficient with the maximum airplane Mach number of 0.65.

The 5-percent rise in C_DS/η near full throttle at 31,000 feet shown in figure 14 is greater than would be expected from the available test data on propellers (references 5 and 6) for a change in forward or tip Mach number of 0.01. Even with consideration of the increase of 10 percent in power coefficient, a decrease in propeller efficiency of not more than 2 percent would be expected. The rise in C_DS/η shown in figure 15 for the same condition is of the same order but the estimated rise in power coefficient is less. If the 3- to 5-percent rise in C_DS/η is actually present as a result of decrease in propeller efficiency, the propeller must be operating in a more critical region with regard to Mach number and power coefficient than any propeller blade form yet tested.

The only appreciable change in operating conditions shown in figure 14 for the full-throttle runs at 31,000 feet is a change in propeller tip Mach number of 0.02. Because

the highest speeds were obtained at the highest free-air temperatures, the airplane Mach number changed little. For the constant propeller rotational speed used, the tip Mach number decreased as the free-air temperature increased. Because the effect on efficiency of change in power coefficient and change in tip Mach number are interrelated, the same conclusions apply to the full-throttle tests as are drawn from the airplane polars.

Additional evidence that the propeller efficiency is affected by operation at high Mach number was obtained by comparison with results of tests at 2700 rpm. Polars obtained at 3000 and at 2700 rpm during the same flight are shown in figures 16 to 19. The reduction in $C_D S/\eta$ due to change in propeller rotational speed from 3000 to 2700 rpm is of the order of 10 percent. Comparison with existing data on propeller efficiencies again indicates that this change is greater by 3 or 4 percent than would be expected, especially in view of the 20 percent increase in power coefficient when operating at 2700 rpm. The fact remains, however, that approximately the same speed was obtained at full throttle at 31,000 feet with 3000 and with 2700 rpm even though the estimated power for 2700 rpm was of the order of 10 percent less. There can be no question of changes in drag coefficient at the same speed and altitude during the same flight; the exact magnitude of the change in propeller efficiency, however, depends on the accuracy of the power estimate.

Evidence of loss in propeller thrust as far inboard as the 0.6 radius at forward Mach numbers as low as 0.66 was found in a pressure survey behind the propeller cuffs reported in reference 7. The conditions of operation were approximately the same as those for the high-speed condition at 31,000 feet, except that the data were taken during a shallow dive.

CONCLUDING REMARKS

In spite of the questionable accuracy of the estimates of power used in the analysis of the data of this report, considerable evidence is presented which indicates that appreciable losses in propeller efficiency were encountered in the maximum level-flight-speed condition due to high propeller Mach number. The gain in maximum

speed obtainable by reducing the propeller rotational speed should be sufficient to warrant a change in propeller reduction gearing from its present value of 0.477 to at least 0.420 as is used on the Merlin 68 engine. This change is comparable to operation at 2700 rpm with the present reduction gearing.

Whether the propeller efficiencies obtainable at the reduced rotational speed are reasonably high cannot be determined definitely unless propeller tests are made with a thrust survey and a torquemeter. It is recommended that this be done in order that the possibility of further improvement can be determined.

Langley Memorial Aeronautical Laboratory
National Advisory Committee for Aeronautics
Langley Field, Va., December 18, 1944

Thomas J. Voglewede
Aeronautical Engineer

Edward C. B. Danforth, III
Aeronautical Engineer

Approved: Melvin N. Gough
Melvin N. Gough
Chief of Flight Research Division

ER

APPENDIX

CALCULATION OF BRAKE HORSEPOWER FROM MEASURED WEIGHT AIR FLOW

If the effects of variation of ignition and port timing with engine speed are ignored and if changes in fuel-air ratio are small enough so as to have a negligible effect on thermal efficiency, the indicated horsepower of an engine may be considered to vary linearly with the amount of air consumed. These conditions are met in the present tests since the effect of changes in fuel-air ratio over the operating range is small and all testing was done with engine speeds of 3000 and 2700 rpm.

The weight flow of charge air was determined by measurement of the pressure difference between the carburetor deck and the boost venturi throat. The carburetor was calibrated by the NACA Aircraft Engine Laboratory at Cleveland, Ohio. The calibration is presented in figure 20 as an adaptation of the method proposed in reference 8 which makes the calibration applicable to any inlet temperature. Because the calibration based on carburetor top-deck pressure was not well defined in the region of maximum power at high blower critical altitude ($\Delta p/P_1$ between 0.50 and 0.60), the calibration based on measurement of carburetor total-head collector shown in figure 20 was used as a guide in fairing the calibration used.

A specific air consumption of 5.7 pounds per indicated horsepower hour was chosen from consideration of dynamometer test data on this engine furnished by Packard Motor Car Company.

The indicated horsepower may be expressed by the following relation:

$$IHP = \frac{W_a}{5.7} = BHP + SHP + FHP - PHP$$

where

IHP indicated horsepower

W_a weight charge-air flow, lb/hr

BHP brake horsepower

SHP horsepower absorbed by the supercharger

FHP friction horsepower

PHP relative net power output of induction and exhaust strokes

The power absorbed by the supercharger was calculated from the impeller tip speed and the mass charge flow, and is given by the following relation based on momentum considerations:

$$SHP = \frac{V_t^2}{550 \times 3600} \times \frac{W_c}{g}$$

where

V_t impeller tip speed, ft/sec

W_c weight charge flow, lb/hr

g acceleration of gravity, ft/sec/sec

Supercharger power computed in this manner agrees well with test data furnished by Packard for a similar supercharger. There will naturally be some slip present which will cause the power absorbed by the supercharger to be overestimated by a few percent. This difference is, however, largely nullified by losses in the gearing. In this case the supercharger power may be overestimated by about 5 percent. This means that the values of brake horsepower may be 1 percent too low.

The friction horsepower was calculated from the following relation which is derived in detail in reference 9:

$$FHP = 15 \times 10^{-10} n_c (l \times N \times d)^2$$

where

n_c number of cylinders

l stroke, in.

N engine speed, rpm

d cylinder diameter, in.

or for this engine

$$FHP = 18.9\left(\frac{N}{1000}\right)^2$$

The pumping power is approximated by the difference in the work done on the piston face by the charge at manifold pressure and the work done by the piston on the exhaust gases at engine back pressure. For these tests the brake horsepower was adjusted for departures from 60 inches of mercury manifold pressure and 30 inches of mercury back pressure. The back pressure was assumed to be equal to the altitude pressure.

$$PHP = \frac{70.73}{33,000}\left(P_{man} - P_S - 30\right)\frac{N}{2} V_d$$

where

P_{man} manifold pressure, in. Hg

P_S altitude pressure, in. Hg

30 reference manifold pressure (60 in. Hg) - reference altitude pressure (30 in. Hg)

N engine speed, rpm

V_d engine displacement, cu ft

This relationship is at best an approximation and may give rise to appreciable inaccuracy in the power estimates where the magnitude and the change in pumping power is large. In these tests, both the manifold pressures and altitude pressures varied over a wide range, and a closer estimate of the pumping power may be necessary for consistent and reasonable results.

The brake horsepower may be calculated from equation (1) by using the results of equations (2), (4), and (5).

The indicated specific air consumption may be expected to vary slightly from low power to high power, because of changes in fuel-air ratio. The fuel-air ratio as determined from the compensated air-metering pressures and the charge-air flow varied between a minimum of 0.075 at the lower powers and a maximum of 0.095 at high powers. This variation would make the estimate of power as much as 2 percent too high in the high-power range and as much as 2 percent too low in the low-power range.

A composite power chart is given in figure 21 with IHP, BHP, and SHP plotted against weight air flow. It is not absolutely correct to plot SHP against weight air flow for this airplane since carburetion is accomplished before the supercharger. The SHP on this chart has been calculated on the basis of air flow and increased in the ratio of 1.085 to account for the weight of the fuel. The fuel-air ratio varies from 0.075 to 0.095 so that the maximum discrepancy in the chart value of SHP will probably not exceed ±1 percent in SHP or approximately ±0.3 percent in BHP.

It is not inferred that brake horsepower calculated by the weight air-flow method is more accurate, as far as general level is concerned, than that obtained from the power charts; the fact that both estimates of power give rise to abnormally low drag coefficients in the low-speed range indicates that neither is accurate. Both estimates are used in the analysis because, in general, the same effects are shown; the difference is principally one of magnitude.

REFERENCES

1. Kelly, Charles H.: Tests of the North American P-51B Airplane in the NACA Full-Scale Tunnel. NACA MR, Army Air Forces, March 15, 1944.

2. Lindsey, W. F.: Effect of Mach Number on Position Error as Applied to a Pitot-Static Tube Located 0.55 Chord Ahead of an Airplane Wing. NACA CB No. L4E29, 1944.

3. Degutis, A. J.: Performance Test of Packard Rolls-Royce V-1650-3 Engine. Memo. Rep. No. ENG-57-503-1011, Materiel Command, Army Air Forces, Oct. 12, 1943.

4. Pinkel, Benjamin, Turner, L. Richard, and Voss, Fred: Design of Nozzles for the Individual Cylinder Exhaust Jet Propulsion System. NACA ACR, April 1941.

5. Stack, John, Draley, Eugene C., Delano, James B., and Feldman, Lewis: Investigation of Two-Blade Propellers at High Forward Speeds in the NACA 8-Foot High-Speed Tunnel.
   I - Effects of Compressibility. NACA 4-308-03 Blade. NACA ACR No. 4A10, 1944.
   II - Effects of Compressibility and Solidity. NACA 4-308-045 Blade. NACA ACR No. 4B16, 1944.

6. Vogeley, A. W.: Climb and High-Speed Tests of a Curtiss No. 714-1C2-12 Four-Blade Propeller on the Republic P-47C Airplane. NACA MR, Army Air Forces, Aug. 31, 1944.

7. Voglewede, T. J.: Pressure Surveys behind the Propeller Cuffs of a P-51B Airplane at Military Power near Maximum Level-Flight Speeds. NACA MR No. L4K02, Army Air Forces, 1944.

8. Voglewede, T. J.: A Proposed Method of Measuring Engine Charge Air Flow in Flight. NACA CB No. L4E25, 1944.

9. Staff of Engine Department: Engine Power at High Altitudes. Rep. No. E.3912, British R.A.E., Dec. 1941.

[redacted]

MR No. L4L18

TABLE I

COMPARISON OF ENGINE PERFORMANCE BEFORE AND AFTER FLIGHT TESTS

		Original Run-In Tests May 31, 1943				
Supercharger gear ratio	Engine speed, rpm	P_{man}, in. Hg	Man. temp., °F	F/A	W_a, lb/hr	Observed bhp
Low	2700	46	168	0.0832	6890	993
High	2700	46	210	.0804	6805	837
Low	3000	61	192	.0891	10190	1367

		Check Run October 2, 1944					
Supercharger gear ratio	Engine speed, rpm	P_{man}, in. Hg	Man. temp. °F	F/A	W_a, lb/hr	Observed bhp	bhp corrected for F/A
Low	2700	46	165	0.0769	7156	990	985
High	2700	46	210	.0766	6777	831	821
Low	3000	61	192	.0828	10302	1381	1364

Note: Before removal from airplane, this engine had accumulated 50 hours and 45 minutes of flight time.

NATIONAL ADVISORY
COMMITTEE FOR AERONAUTICS

[redacted]

FIGURE LEGENDS

Figure 1.- Front view of P-51B airplane.

Figure 2.- Three-quarter front view of P-51B airplane.

Figure 3.- Side view of P-51B airplane.

Figure 4.- Three-quarter rear view of P-51B airplane.

Figure 5.- Rear view of P-51B airplane.

Figure 6.- Free air resistance bulb thermometer installation and seals over wing gun ports and wing fittings.

Figure 7.- Special short-boom airspeed head.

Figure 8.- Flight calibration of free air temperature installation.

Figure 9.- Position error of static pressure of short boom airspeed head.

Figure 10.- Variation of weight air flow with indicated horsepower at 3000 rpm based on Wright Field power charts and carburetor air temperature.

Figure 11.- Effect of density on performance near high blower critical altitude. Brake horsepower from measured charge air flow.

Figure 12.- Effect of density on performance near high blower critical altitude. Brake horsepower from power charts.

Figure 13.- Variation of free air temperature with altitude for initial high speed flights near high blower critical altitude.

Figure 14.- Airplane polars at a series of altitudes. Brake horsepower from measured charge air flow.

Figure 14.- Concluded.

Figure 15.- Airplane polars at a series of altitudes. Brake horsepower from power charts.

FIGURE LEGENDS - Concluded

Figure 16.- Effect of reducing propeller tip speed at 31,000 feet pressure altitude. Brake horsepower from measured charge air flow.

Figure 17.- Effect of reducing propeller tip speed at 31,000 feet pressure altitude. Brake horsepower from power charts.

Figure 18.- Effect of reducing propeller tip speed at 31,000 feet pressure altitude. Brake horsepower from measured charge air flow.

Figure 18.- Concluded.

Figure 19.- Effect of reducing propeller tip speed at 31,000 feet pressure altitude. Brake horsepower from power charts.

Figure 20.- Calibration of Bendix-Stromberg PD18A1 carburetor serial number 142204.

Figure 21.- Power chart based on the measured weight charge air flow.

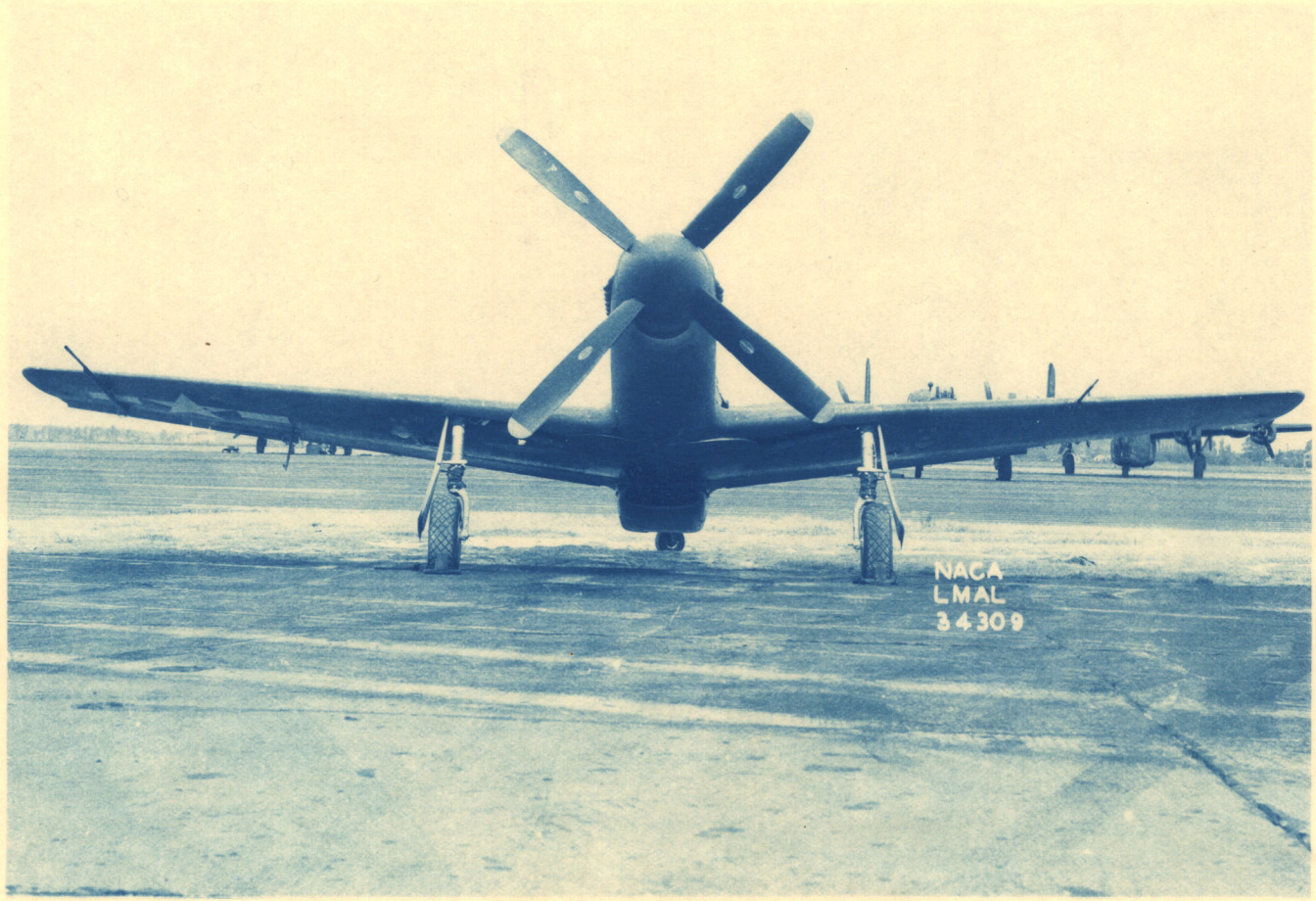

Figure 1.- Front view of P-51B airplane.

NATIONAL ADVISORY COMMITTEE FOR AERONAUTICS
LANGLEY MEMORIAL AERONAUTICAL LABORATORY - LANGLEY FIELD, VA.

MR No. L4L18

CONFIDENTIAL

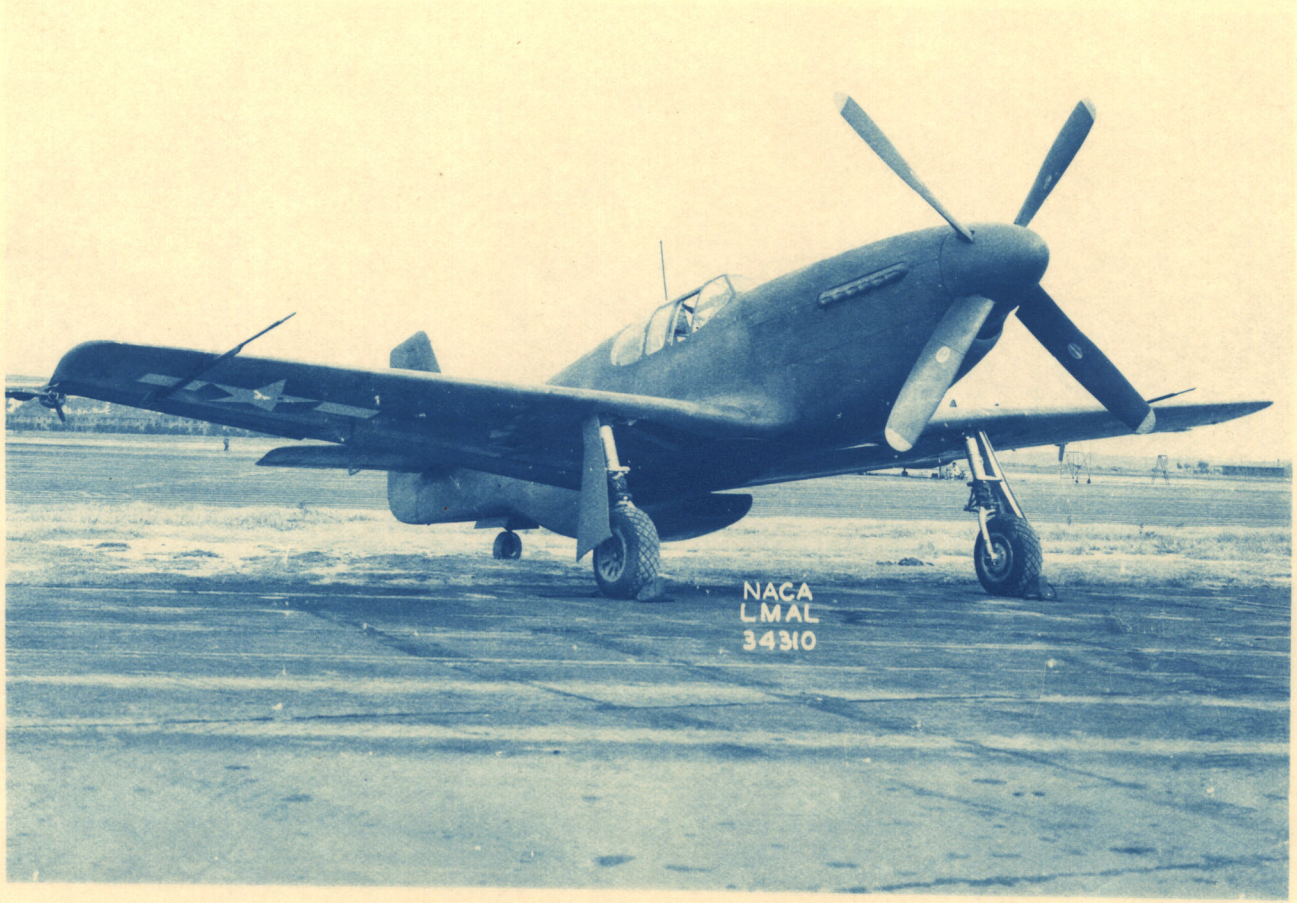

Figure 2.- Three-quarter front view of P-51B airplane.

NATIONAL ADVISORY COMMITTEE FOR AERONAUTICS
LANGLEY MEMORIAL AERONAUTICAL LABORATORY - LANGLEY FIELD, VA.

CONFIDENTIAL

MR No. L4L18

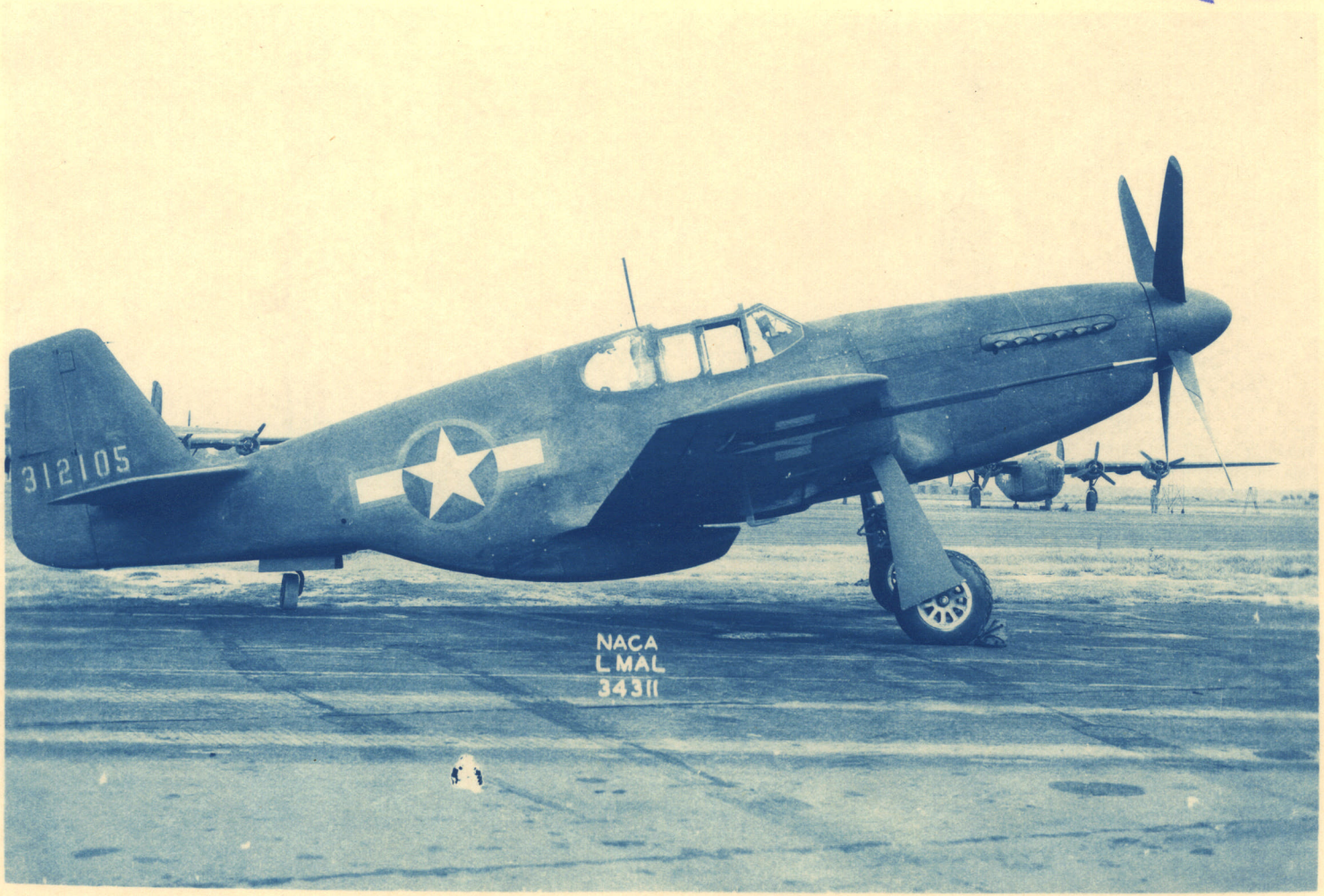

Figure 3.- Side view of P-51B airplane.

NATIONAL ADVISORY COMMITTEE FOR AERONAUTICS
LANGLEY MEMORIAL AERONAUTICAL LABORATORY - LANGLEY FIELD, VA.

MR No. L4I18

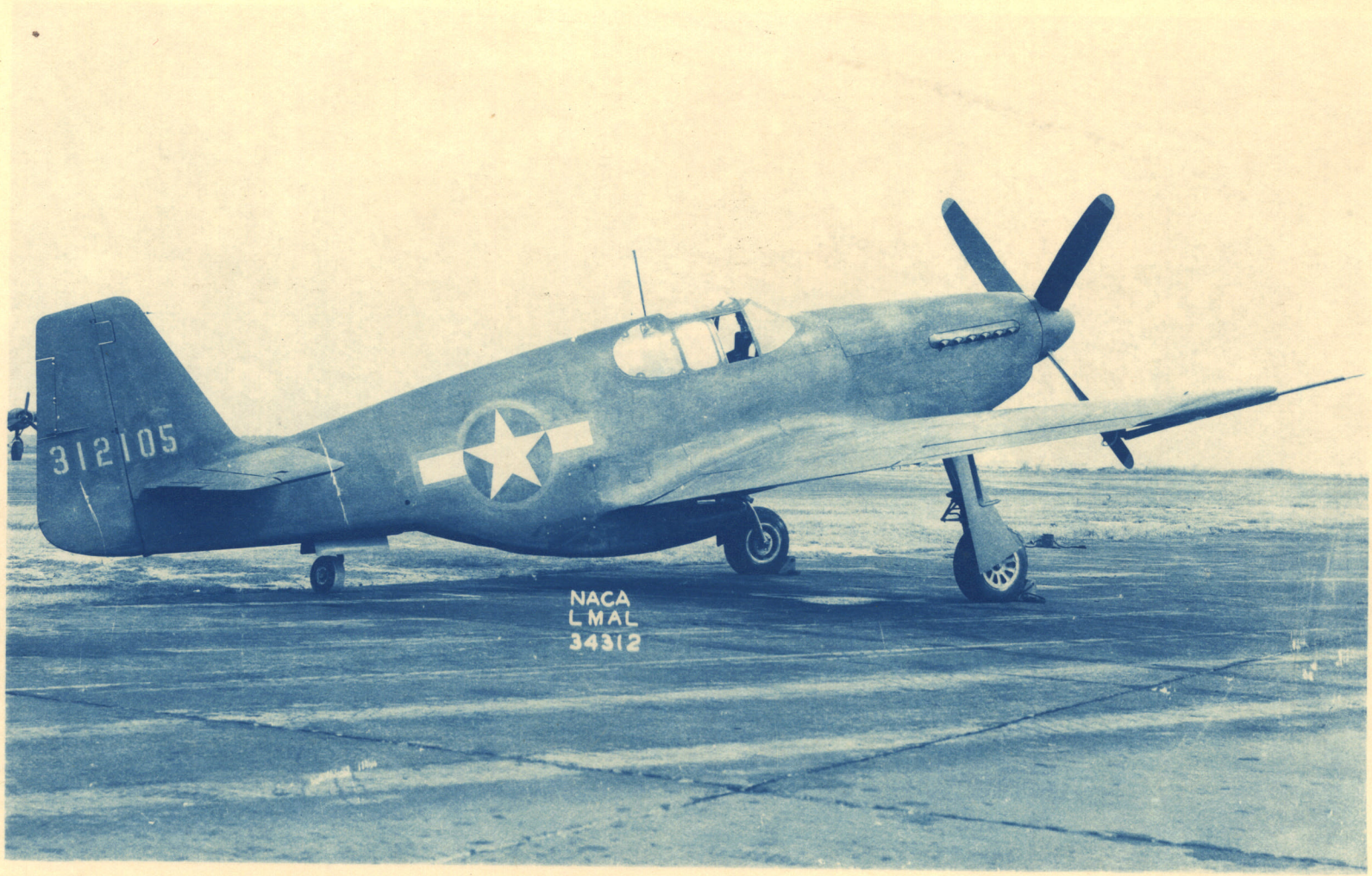

Figure 4.- Three-quarter rear view of P-51B airplane.

NATIONAL ADVISORY COMMITTEE FOR AERONAUTICS
LANGLEY MEMORIAL AERONAUTICAL LABORATORY - LANGLEY FIELD, VA.

MR No. L4L18

CONFIDENTIAL

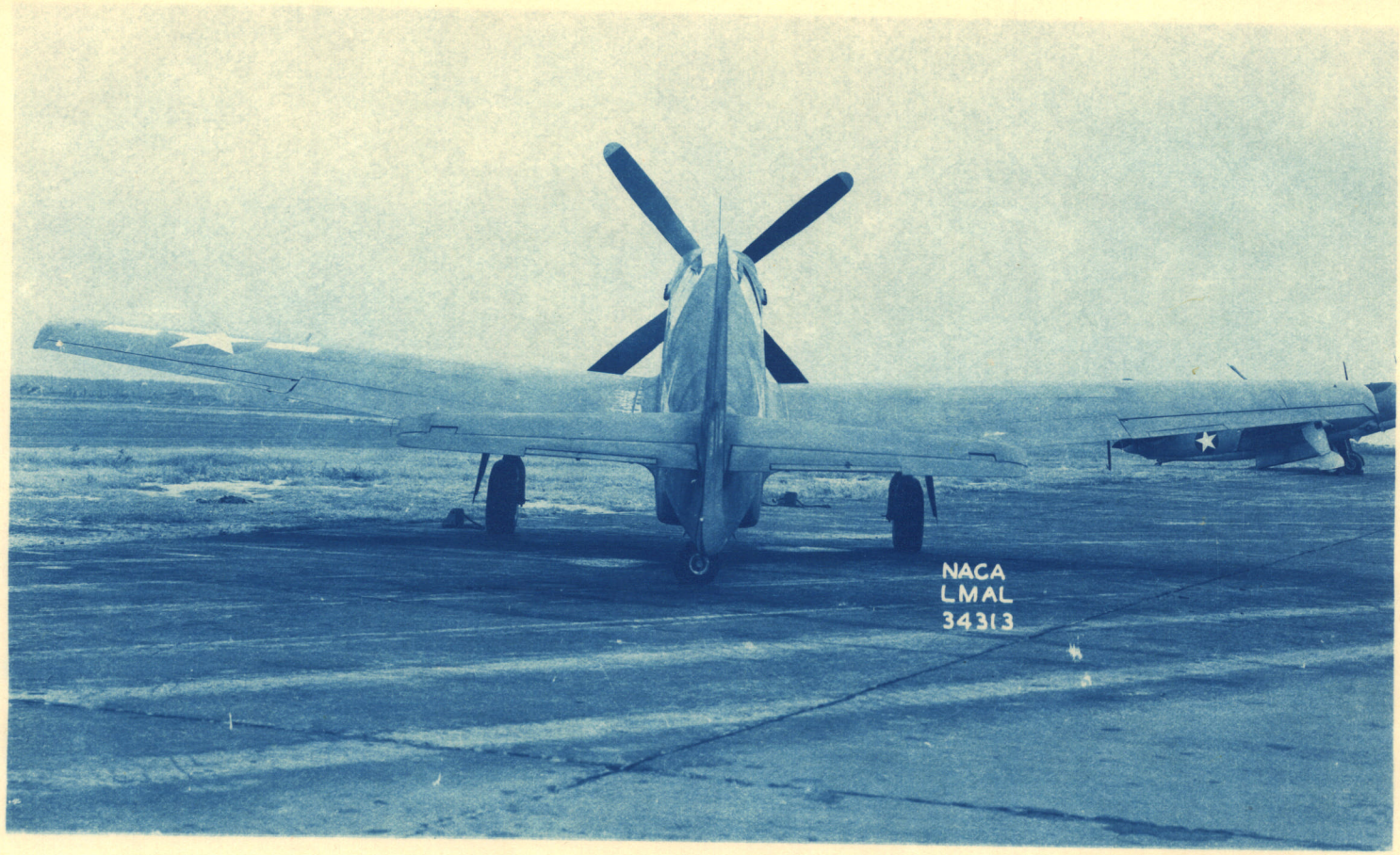

Figure 5.- Rear view of P-51B airplane.

CONFIDENTIAL

NATIONAL ADVISORY COMMITTEE FOR AERONAUTICS
LANGLEY MEMORIAL AERONAUTICAL LABORATORY - LANGLEY FIELD, VA.

CONFIDENTIAL

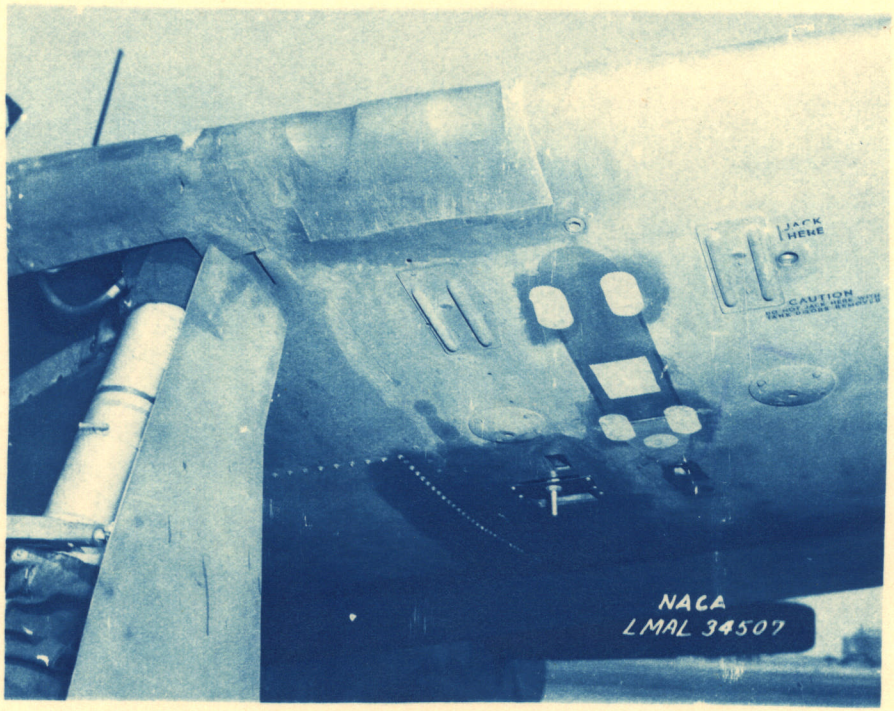

MR No. L4L18

Figure 6.- Free air resistance bulb thermometer installation and seals over wing gun ports and wing fittings.

CONFIDENTIAL

NATIONAL ADVISORY COMMITTEE FOR AERONAUTICS
LANGLEY MEMORIAL AERONAUTICAL LABORATORY - LANGLEY FIELD, VA.

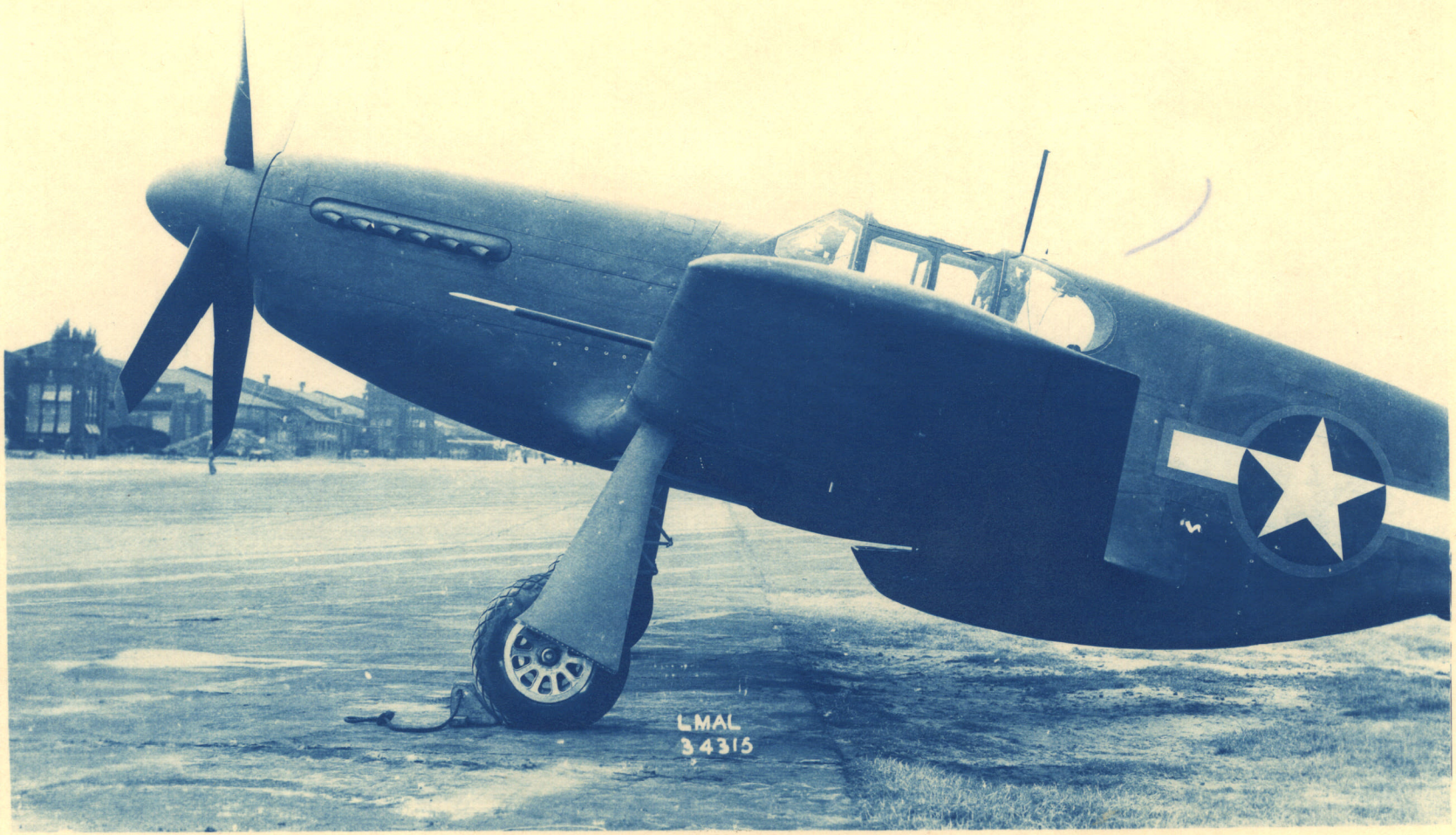

Figure 7.- Special short-boom airspeed head.

NATIONAL ADVISORY COMMITTEE FOR AERONAUTICS
LANGLEY MEMORIAL AERONAUTICAL LABORATORY - LANGLEY FIELD, VA.

MR No. L4L18

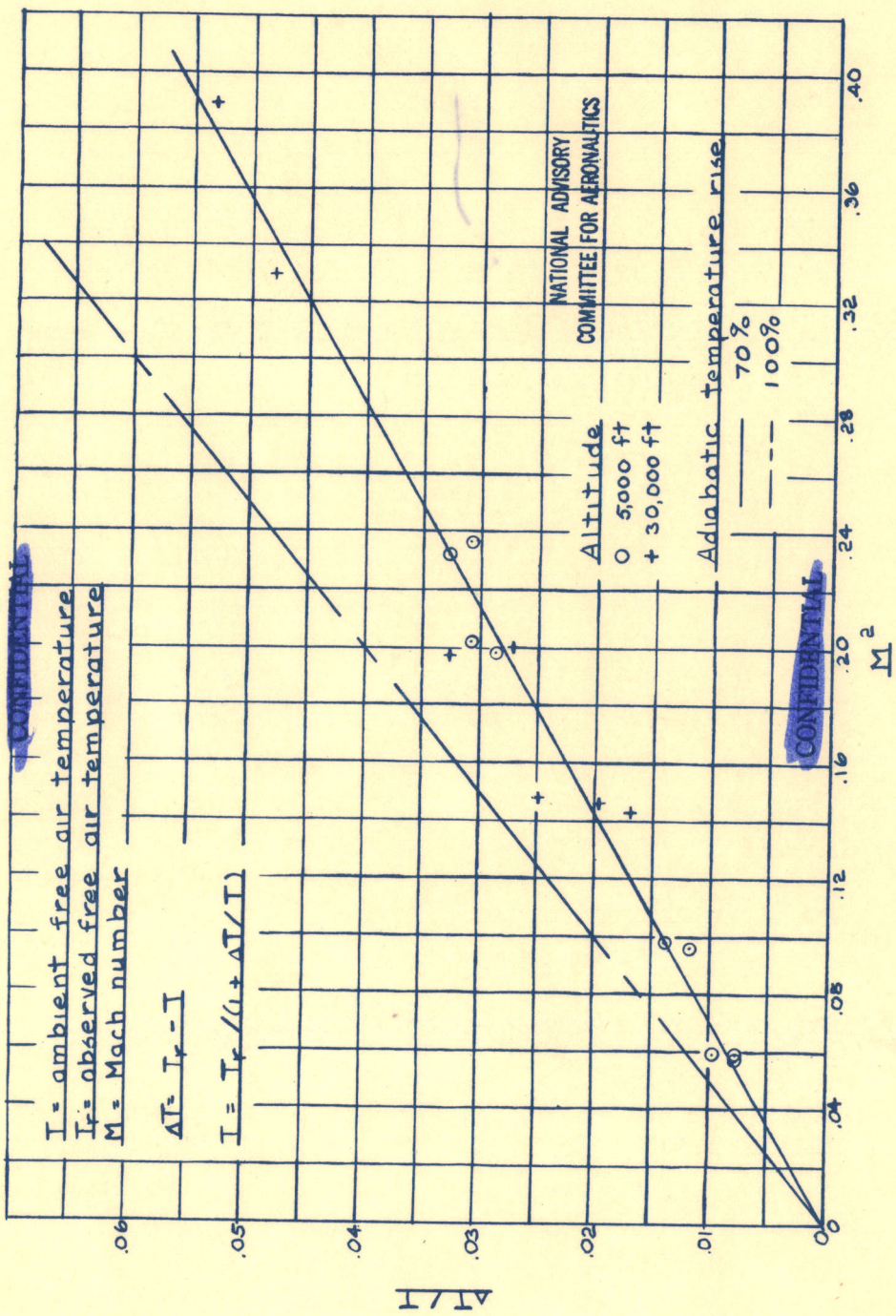

Figure 8.- Flight calibration of free air temperature installation.

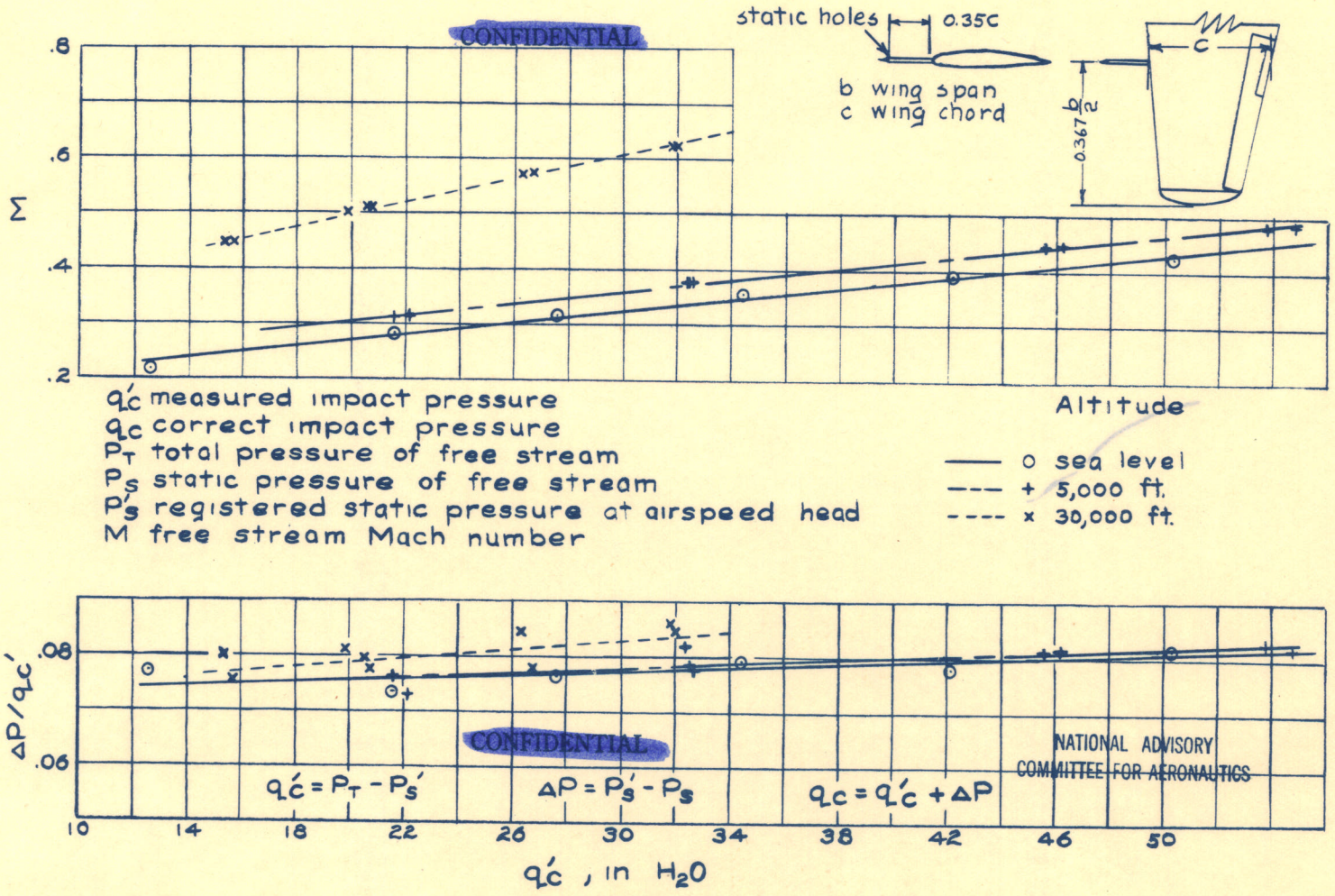

Figure 9.- Position error of static pressure of short boom airspeed head.

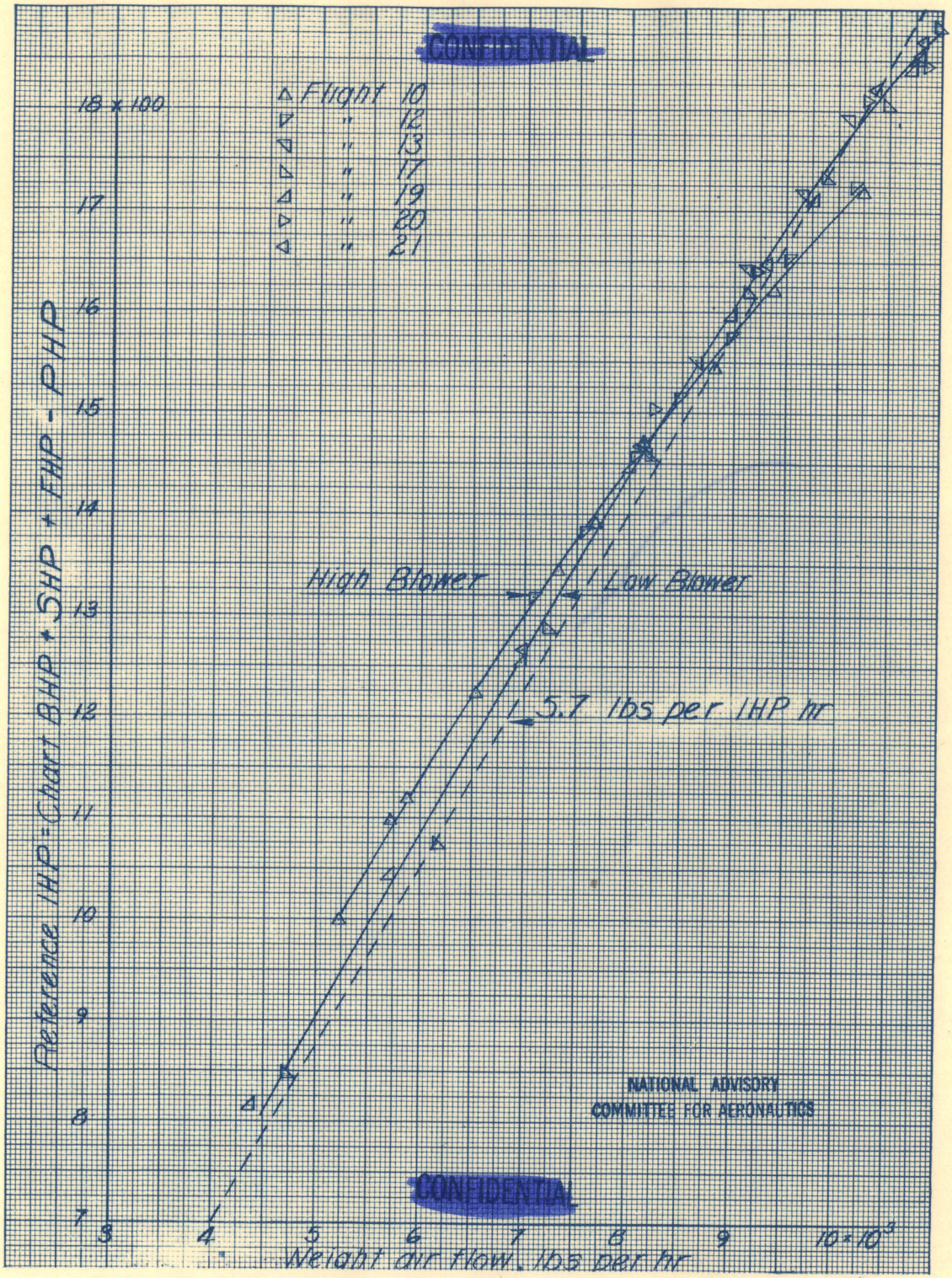

Figure 10.- Variation of weight air flow with indicated horsepower at 3000 rpm based on Wright Field power charts and carburetor air temperature.

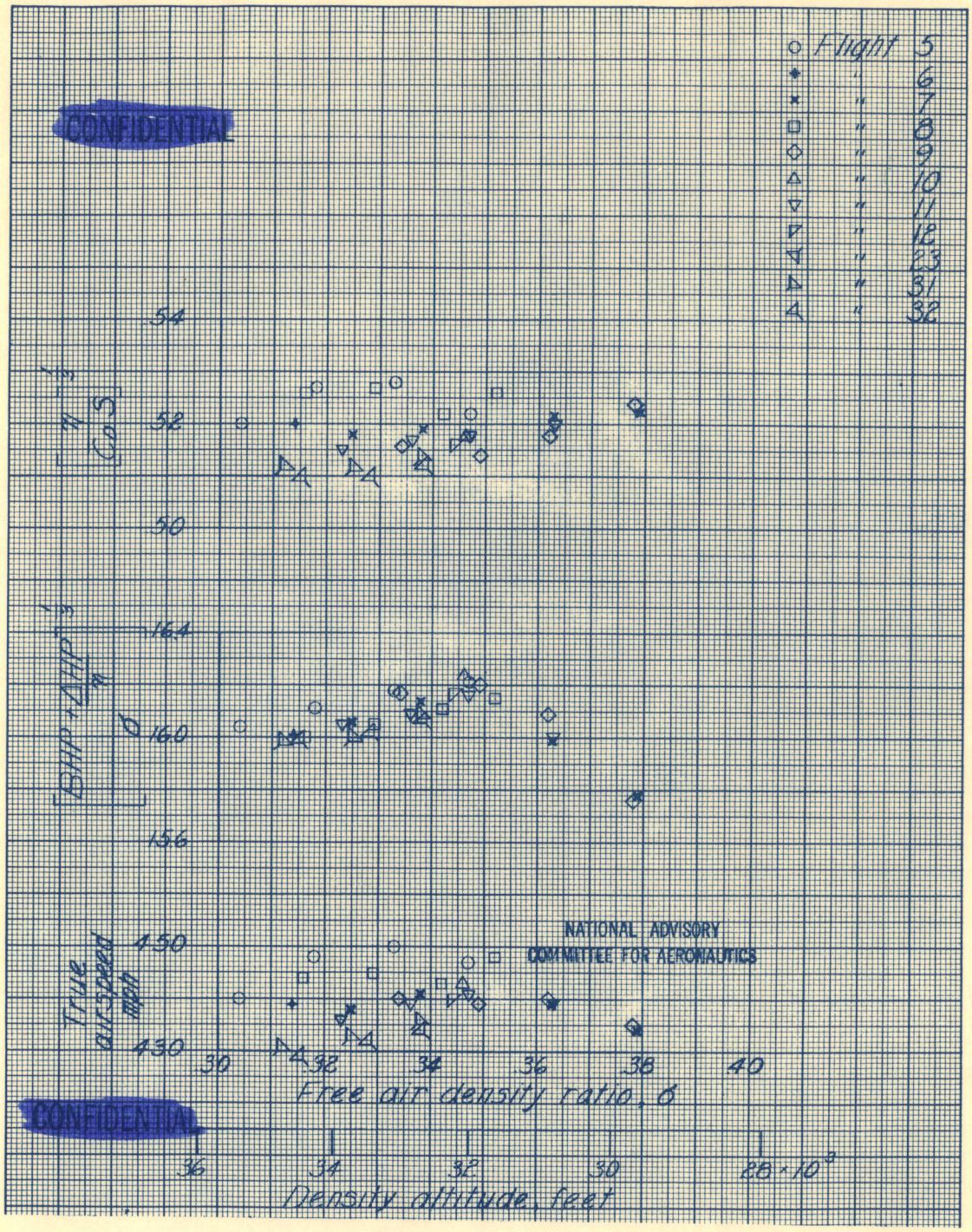

Figure 11.- Effect of density on performance near high blower critical altitude. Brake horsepower from measured charge air flow.

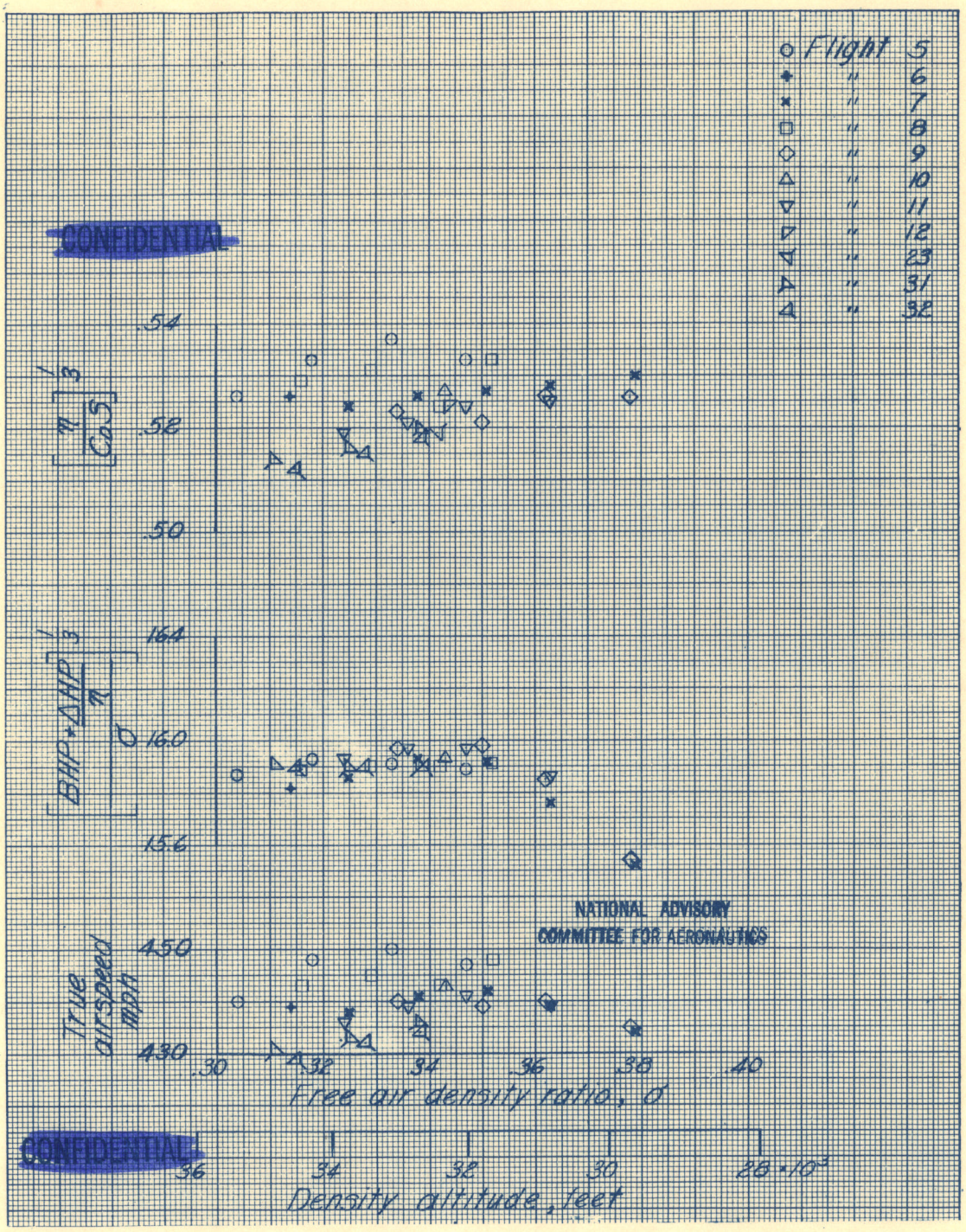

Figure 12.- Effect of density on performance near high blower critical altitude. Brake horsepower from power charts.

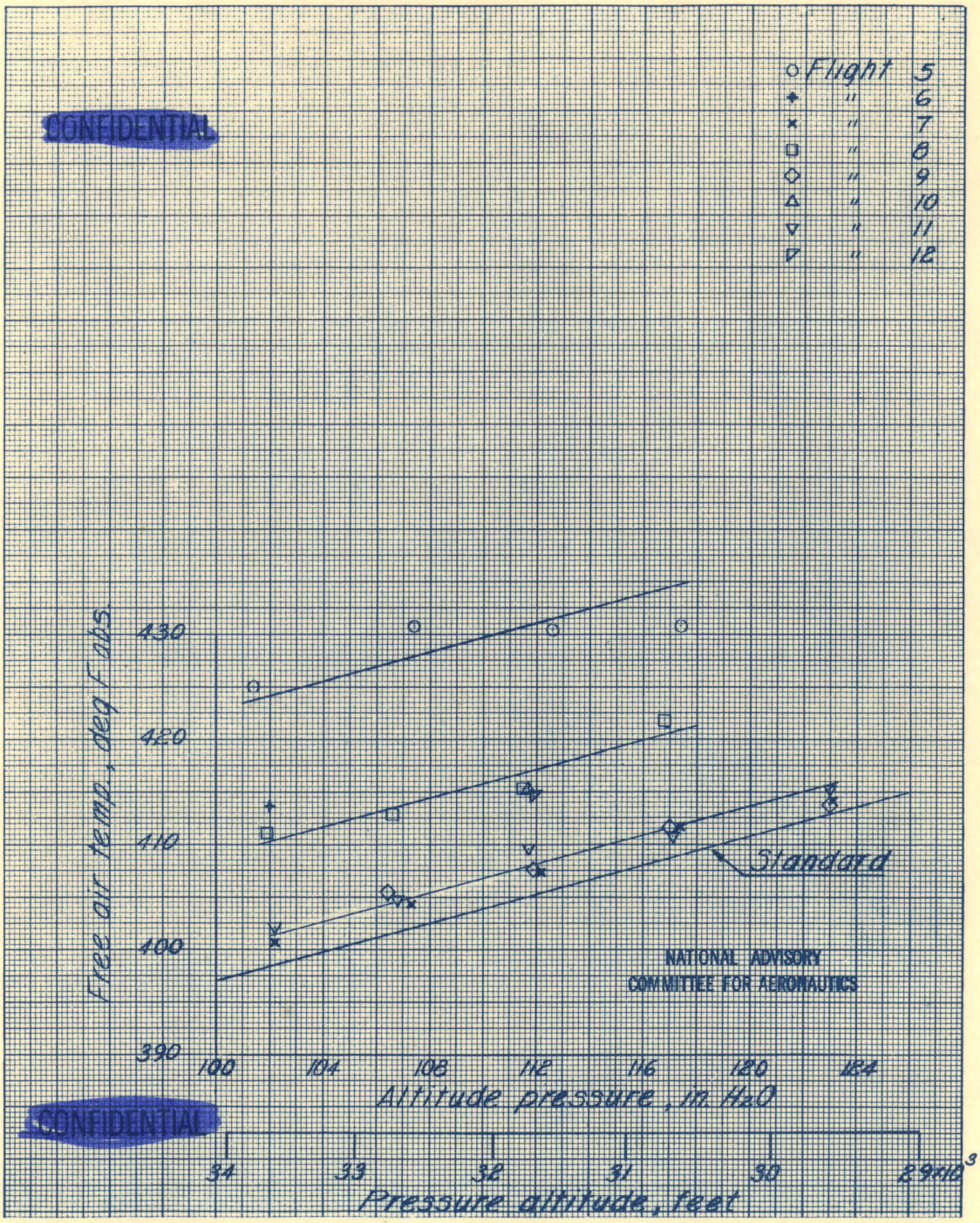

Figure 13.- Variation of free air temperature with altitude for initial high speed flights near high blower critical altitude.

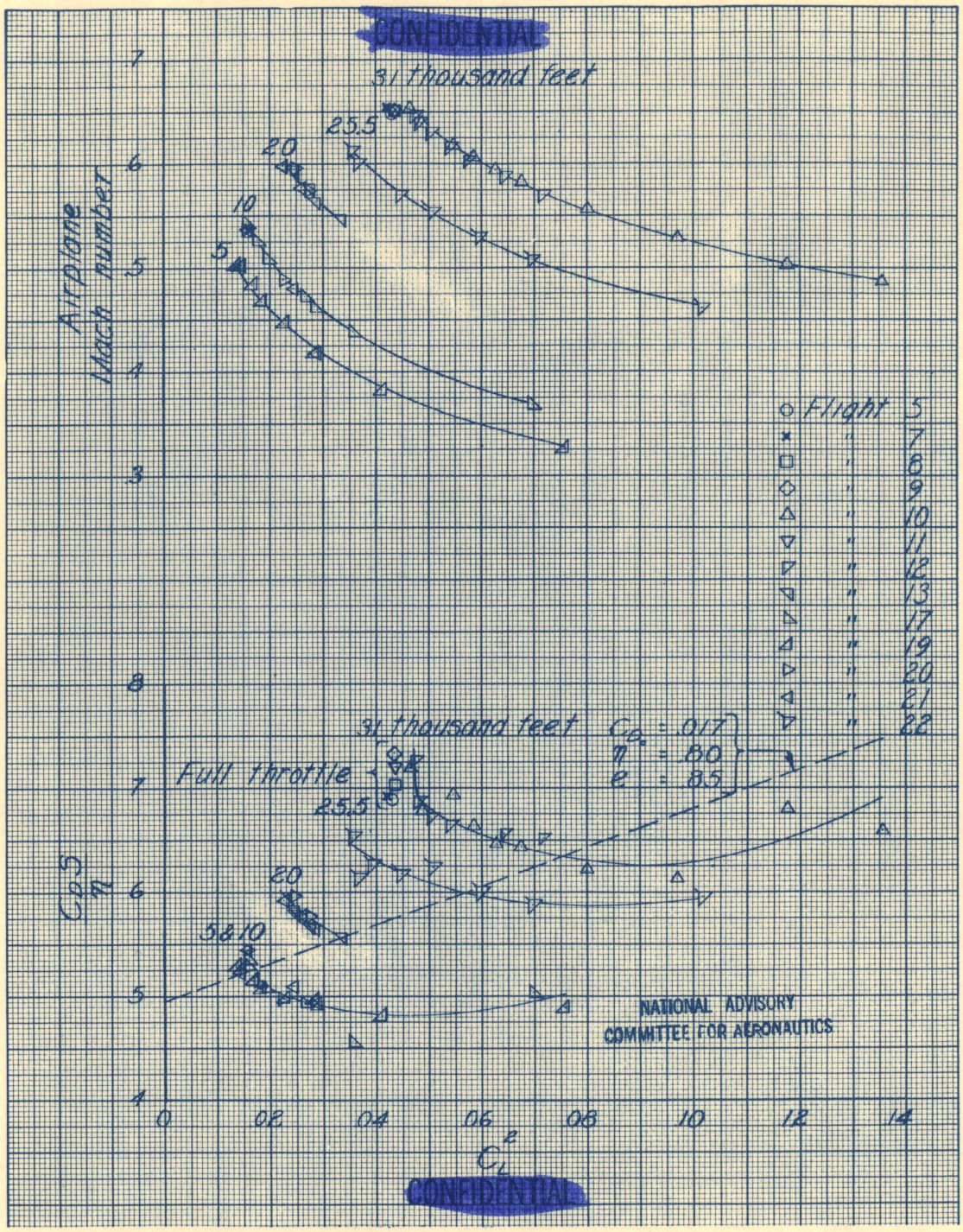

Figure 14.- Airplane polars at a series of altitudes. Brake horsepower from measured charge air flow.

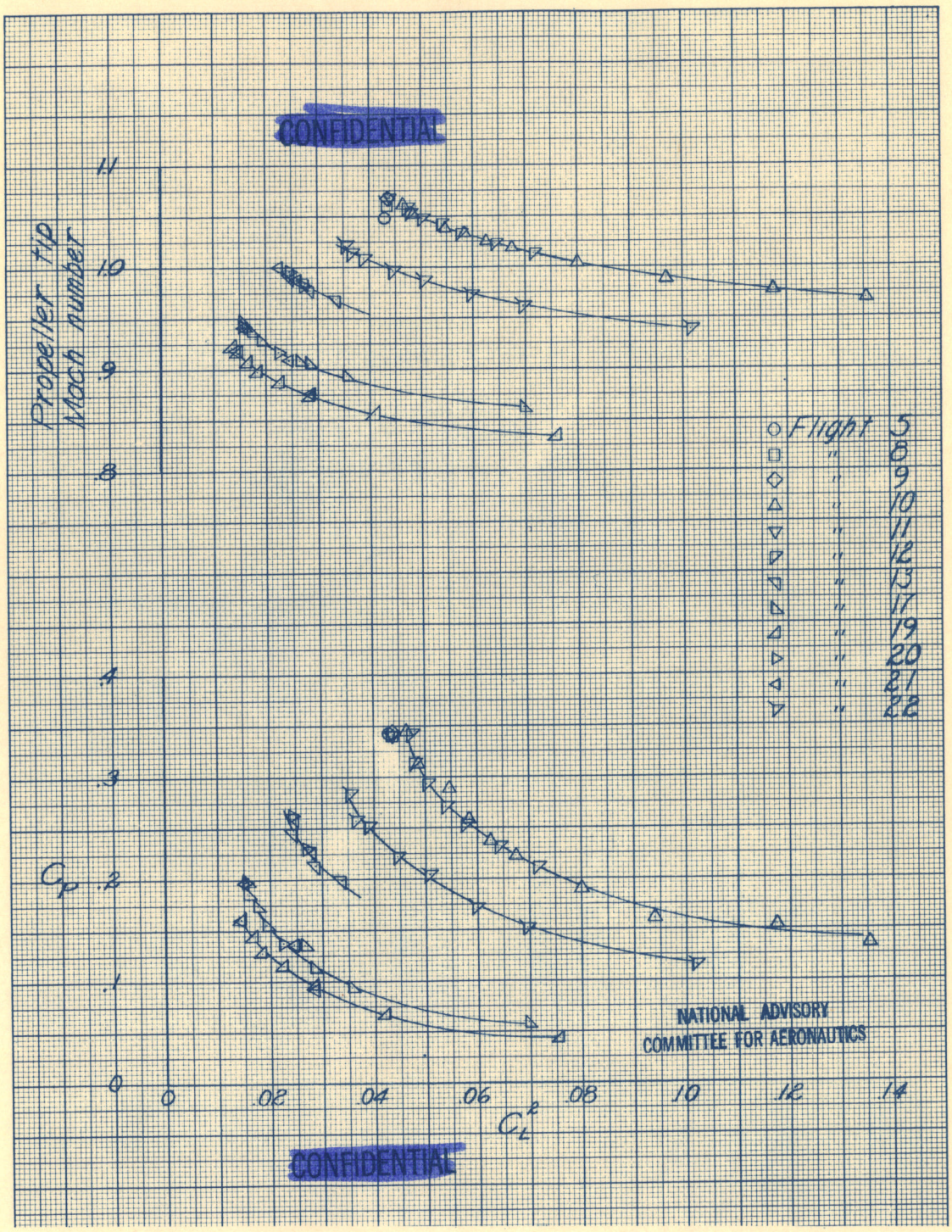

Figure 14.- Concluded.

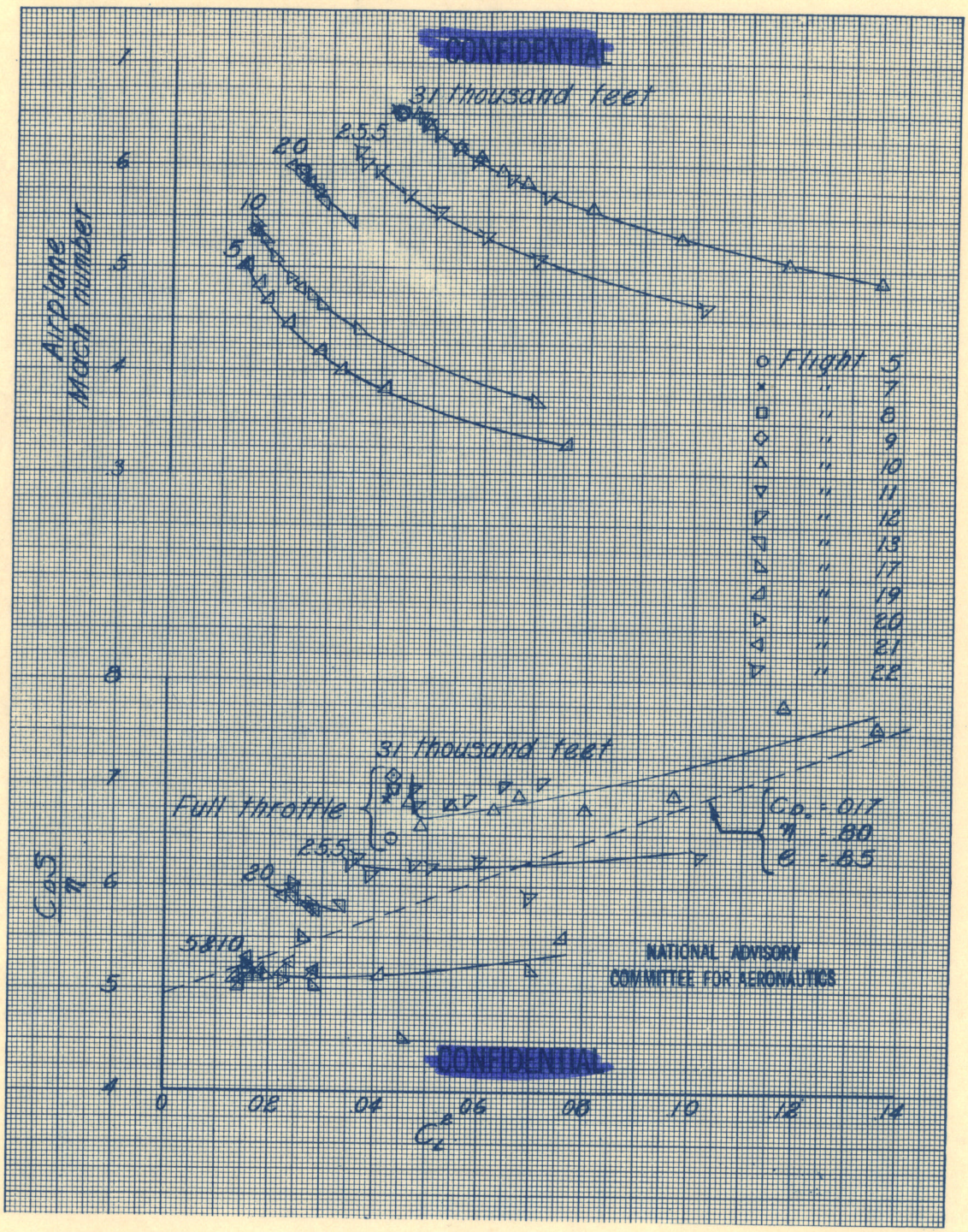

Figure 15.- Airplane polars at a series of altitudes. Brake horsepower from power charts.

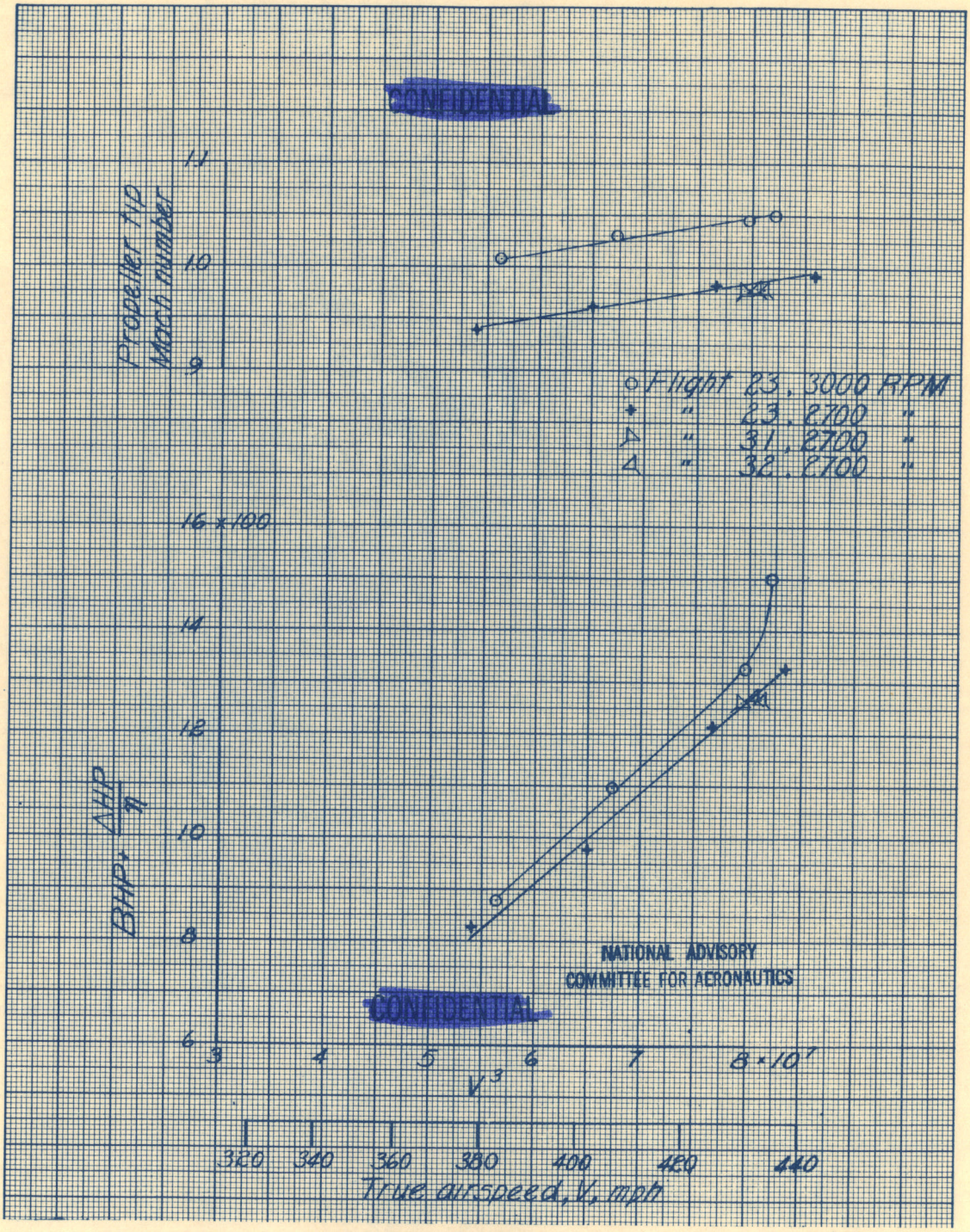

Figure 16.- Effect of reducing propeller tip speed at 31,000 feet pressure altitude. Brake horsepower from measured charge air flow.

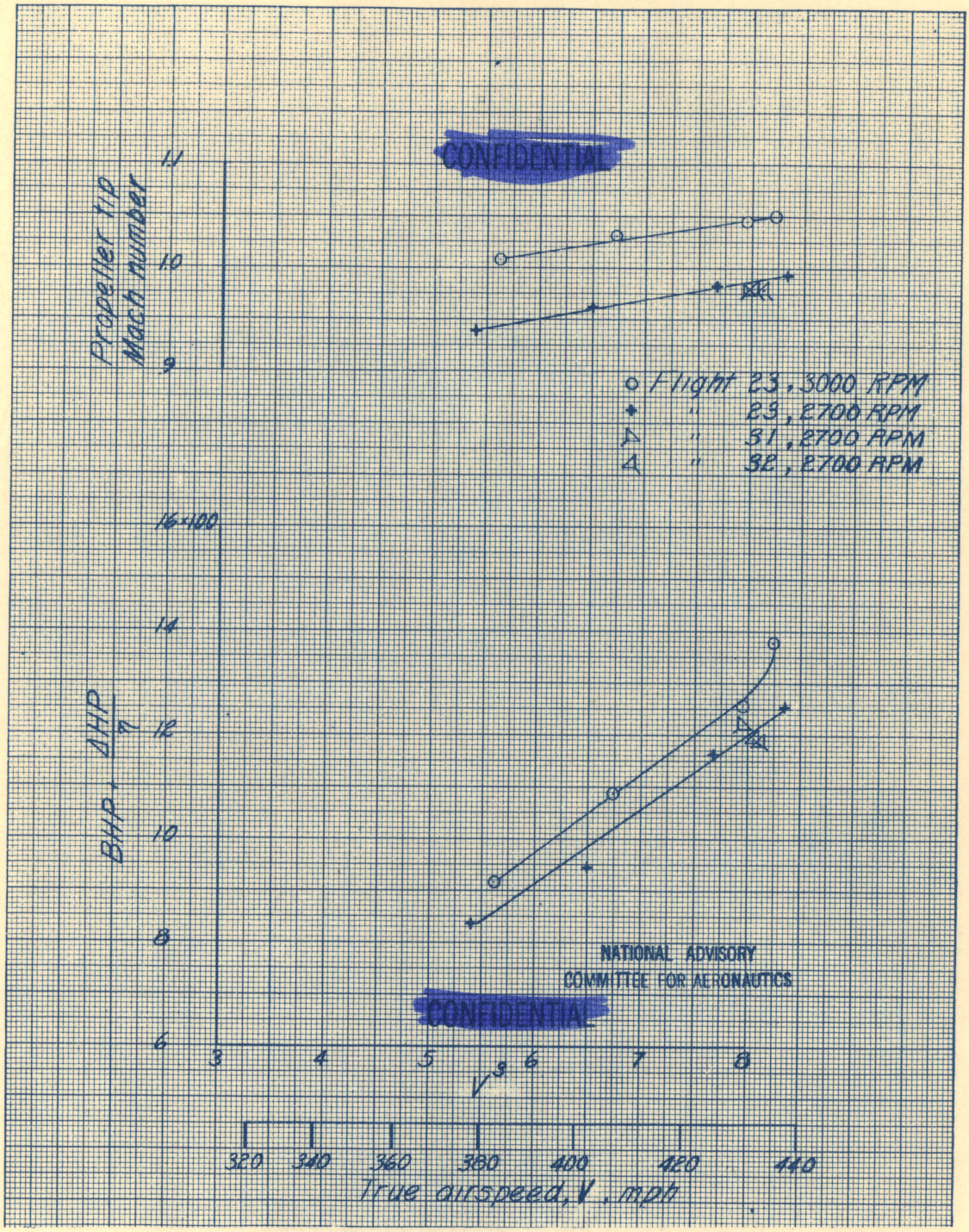

Figure 17.- Effect of reducing propeller tip speed at 31,000 feet pressure altitude. Brake horsepower from power charts.

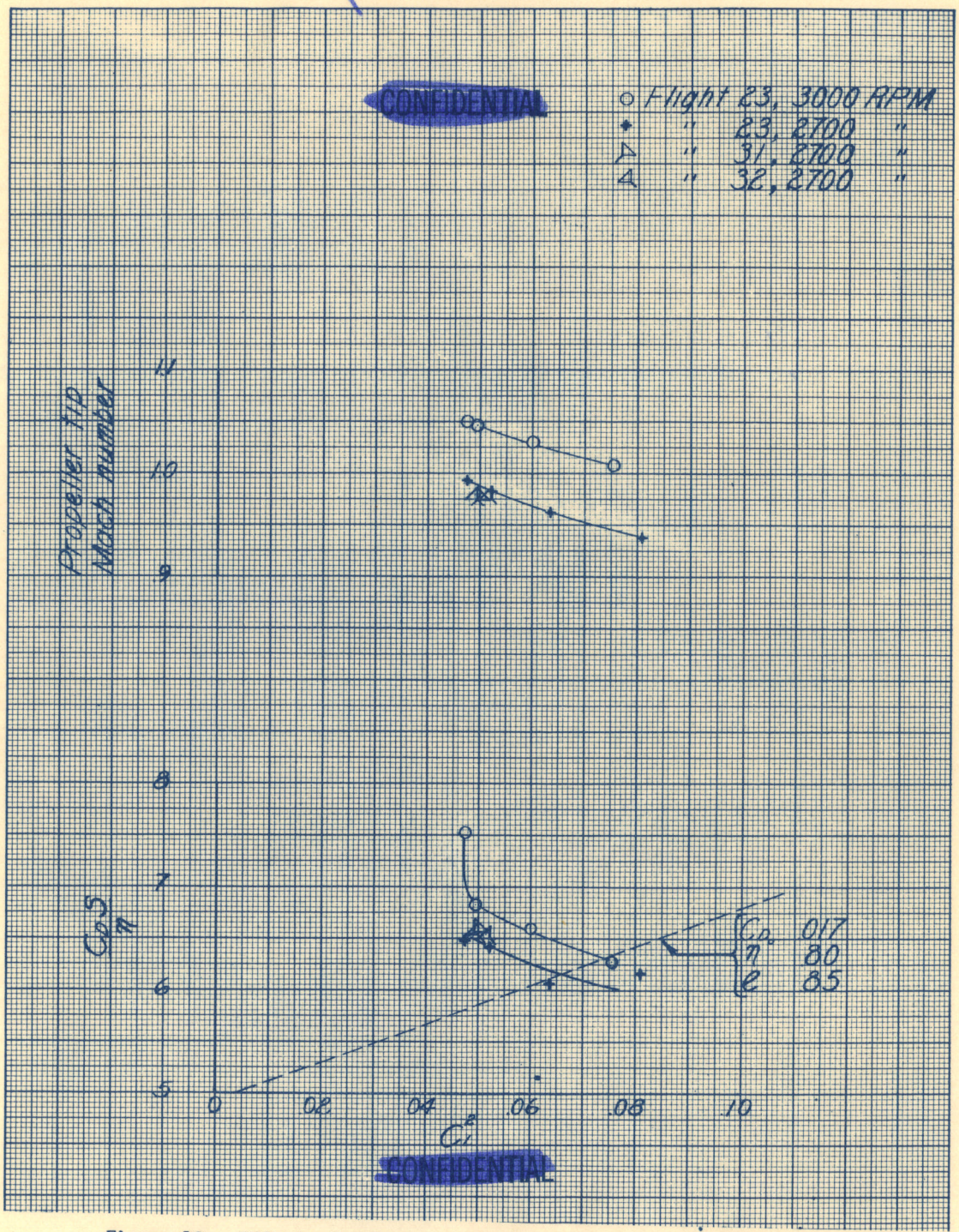

Figure 18.- Effect of reducing propeller tip speed at 31,000 feet pressure altitude. Brake horsepower from measured charge air flow.

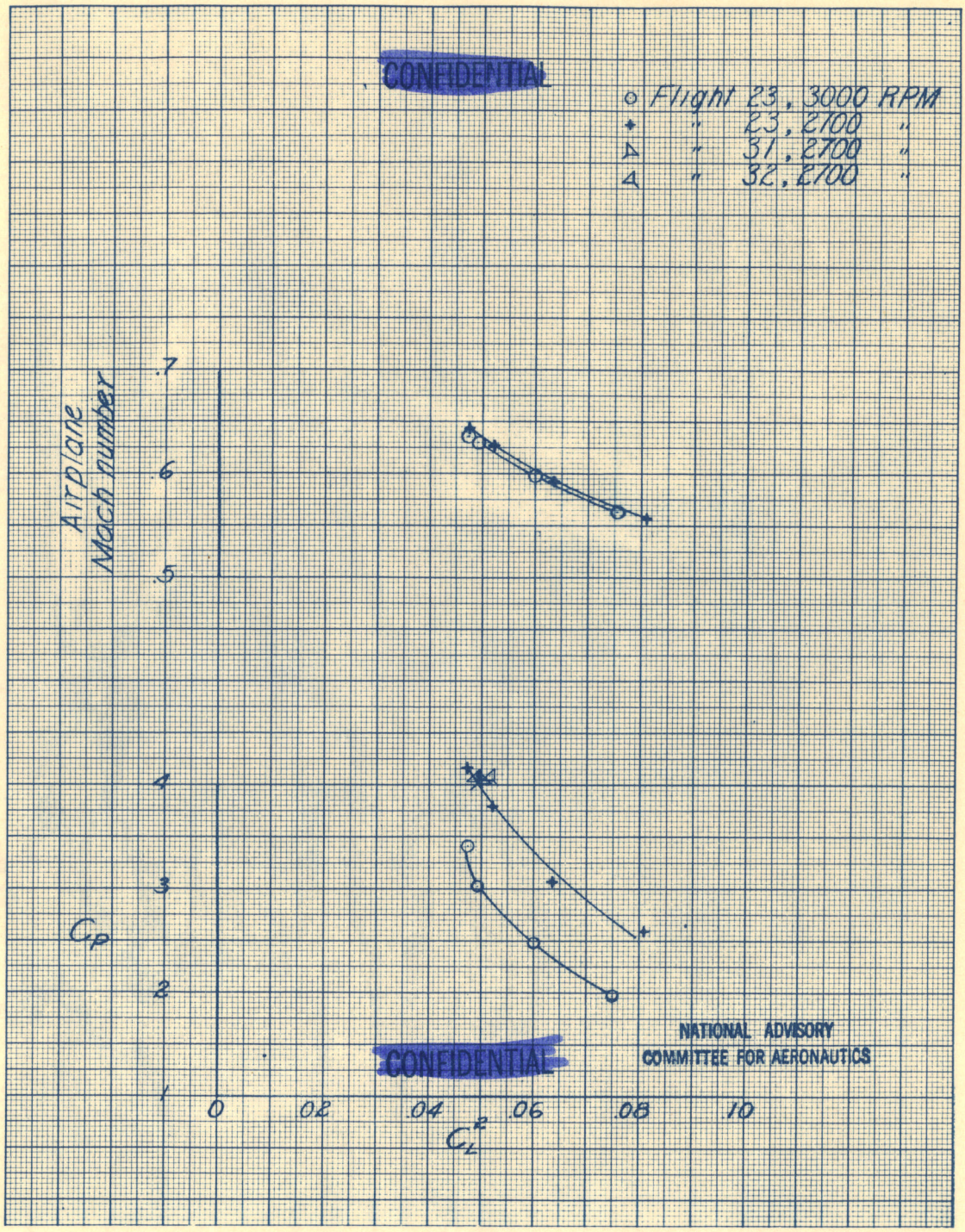

Figure 18.- Concluded.

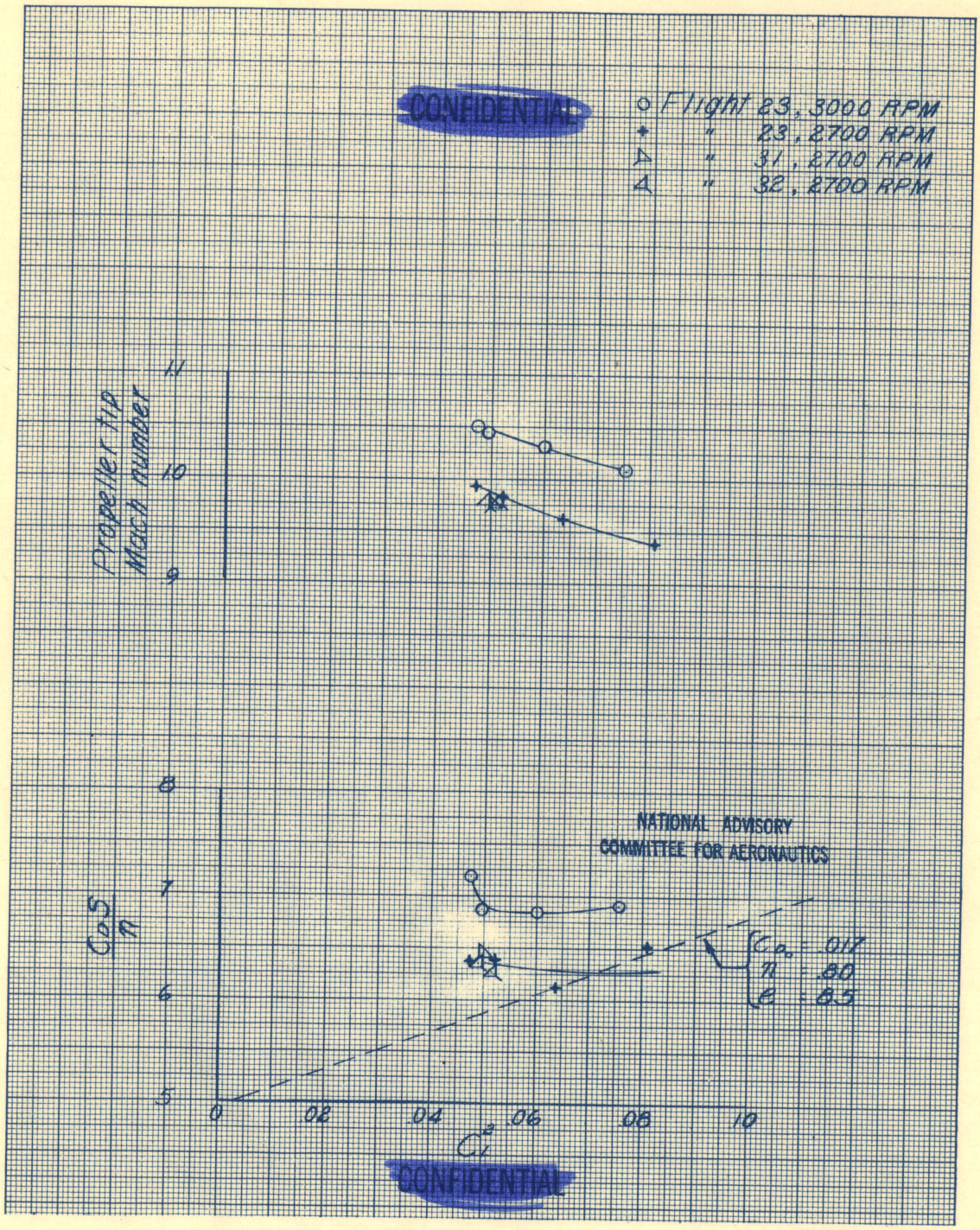

Figure 19.- Effect of reducing propeller tip speed at 31,000 feet pressure altitude. Brake horsepower from power charts.

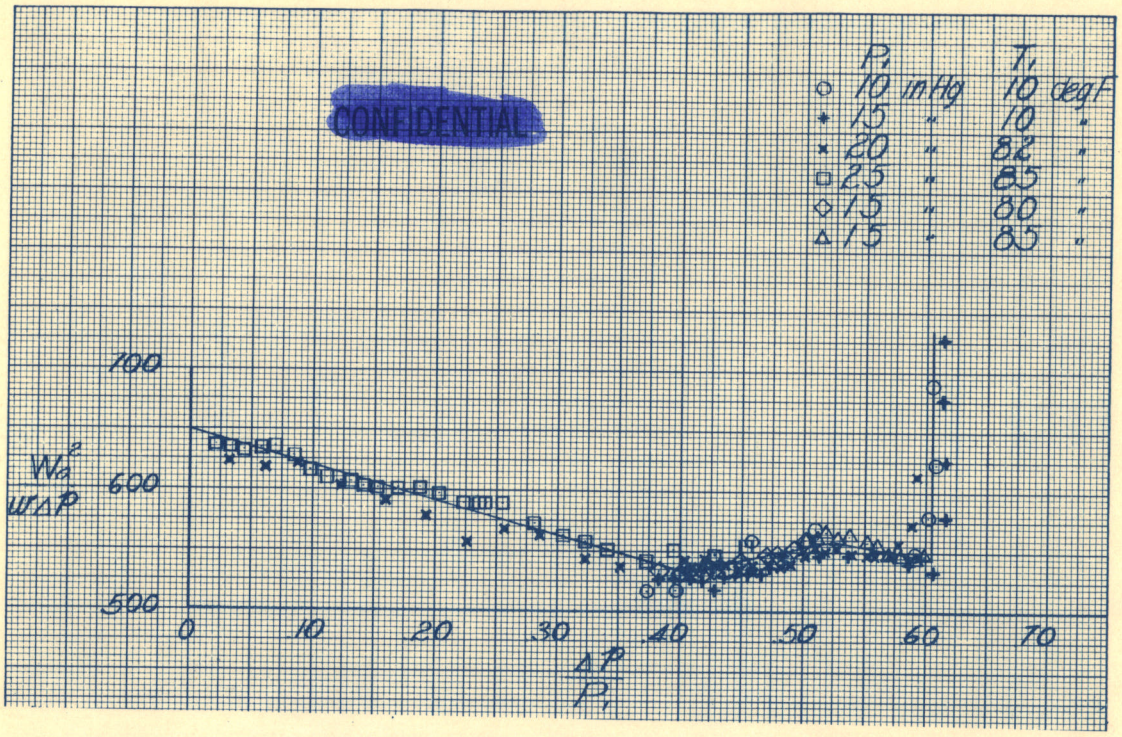

(a) Referenced to total head collector pressure.

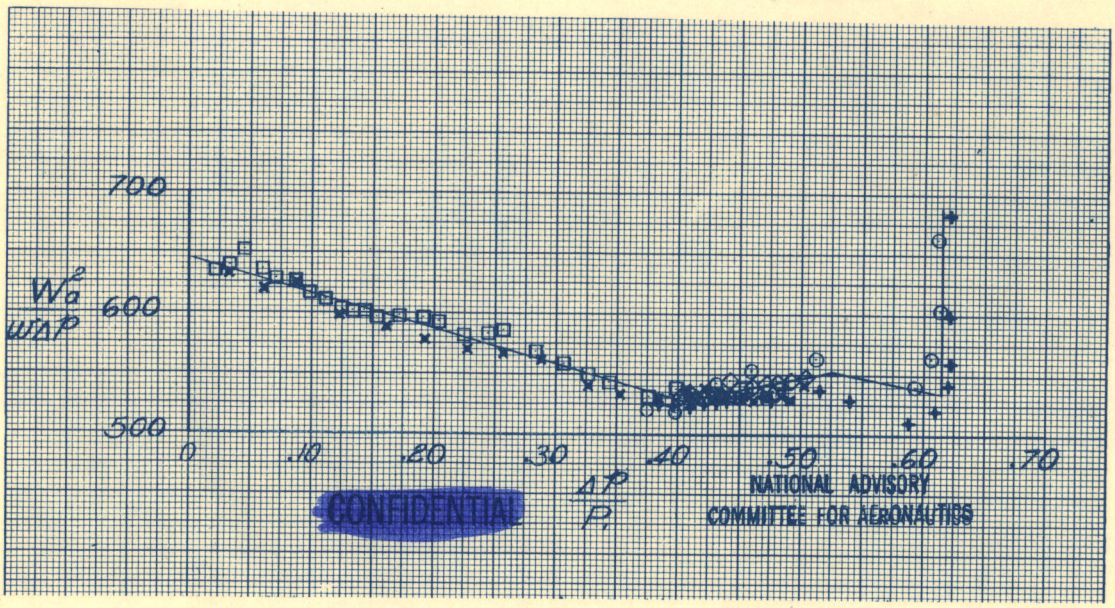

(b) Referenced to top deck static pressure.

Figure 20.- Calibration of Bendix-Stromberg PD18A1 carburetor serial number 142204.

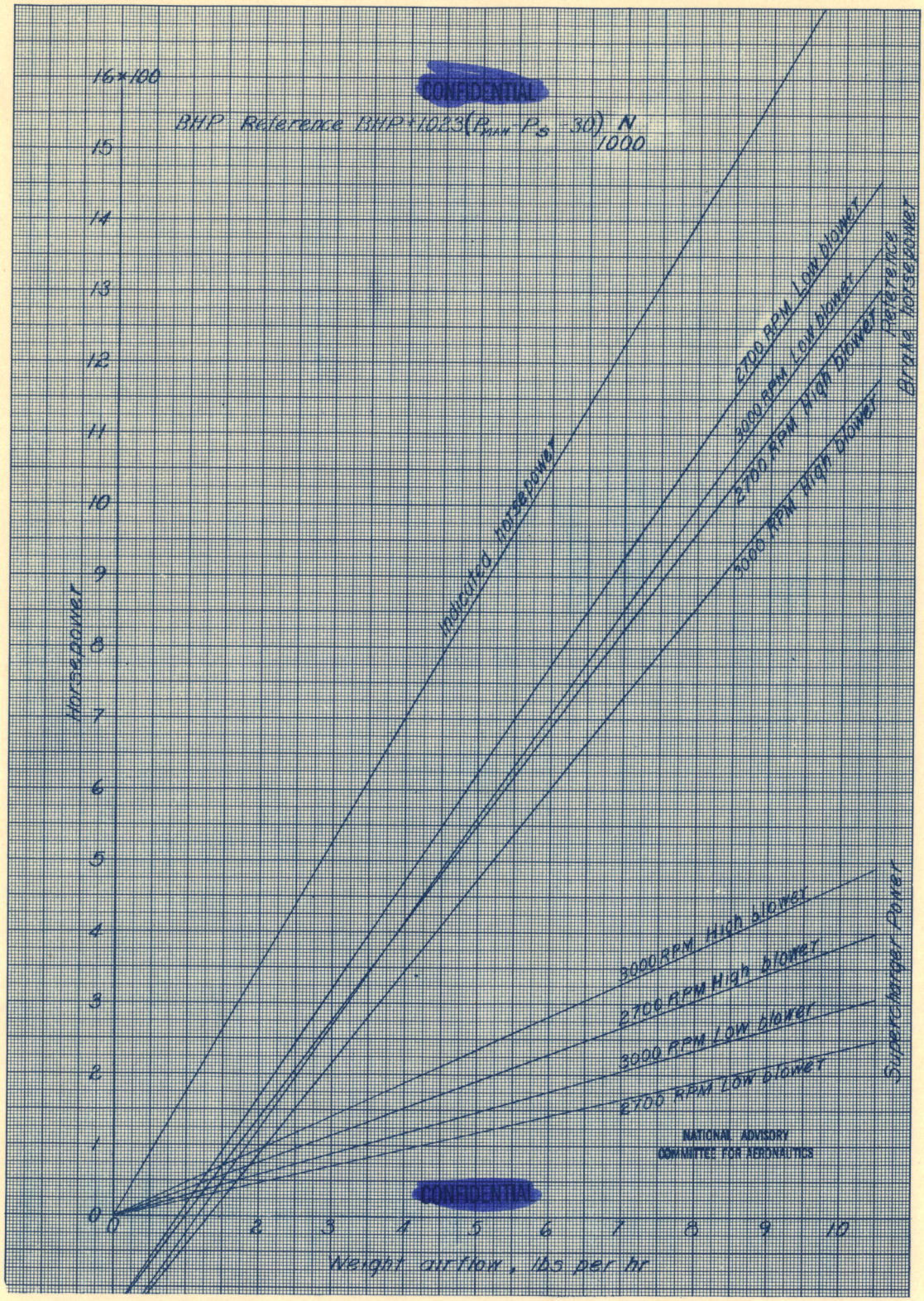

Figure 21.- Power chart based on the measured weight charge air flow.